NACA

RESEARCH MEMORANDUM

EFFECTS OF LEADING-EDGE RADIUS ON THE LONGITUDINAL STABILITY OF TWO 45° SWEPTBACK WINGS INCORPORATING LEADING-EDGE CAMBER AS INFLUENCED BY REYNOLDS NUMBERS UP TO 8.00×10^6 AND MACH NUMBERS UP TO 0.290

By Gerald V. Foster

Langley Aeronautical Laboratory
Langley Field, Va.

NATIONAL ADVISORY COMMITTEE
FOR AERONAUTICS

WASHINGTON

October 6, 1955

NATIONAL ADVISORY COMMITTEE FOR AERONAUTICS

RESEARCH MEMORANDUM

EFFECTS OF LEADING-EDGE RADIUS ON THE LONGITUDINAL STABILITY OF TWO 45° SWEPTBACK WINGS INCORPORATING LEADING-EDGE CAMBER AS INFLUENCED BY REYNOLDS NUMBERS UP TO 8.00×10^6 AND MACH NUMBERS UP TO 0.290

By Gerald V. Foster

SUMMARY

Results of tests conducted in the Langley 19-foot pressure tunnel to determine the low-speed longitudinal stability characteristics of two cambered 45° sweptback wings (aspect ratios of 3 and 5) and the associated effects of camber, leading-edge radius, Reynolds number, and Mach number are presented herein. The wing airfoil sections are defined by an NACA 0009 thickness distribution and a 230 mean line modified for a design lift coefficient of 0.4. Tests were conducted at tunnel pressures of 14.7 and 33 pounds per square inch, which permitted ranges of Reynolds number from 1.14×10^6 to 5.50×10^6 and from 1.80×10^6 to 8.00×10^6 with corresponding ranges of Mach number from 0.058 to 0.290 and from 0.024 to 0.204, respectively.

In general, an increase in leading-edge radius from 0.25 to 0.89 percent chord, the addition of camber, or an increase in Reynolds number for a constant Mach number resulted mainly in a delay to a higher lift coefficient of marked destabilizing changes in the pitching-moment characteristics. An increase in Mach number for a Reynolds number of 5.00×10^6 resulted in a decrease in the lift coefficient at which destabilizing changes of the aspect-ratio-3 wing occurred but had no appreciable effect on the stability characteristics of the aspect-ratio-5 wing. The Mach number effects were, on the whole, appreciably less than were found for uncambered wings.

INTRODUCTION

A general investigation of the effects of systematic changes of wing geometric parameters on the static longitudinal stability and surface flow characteristics of sweptback wings is currently being conducted in the Langley 19-foot pressure tunnel. The initial tests reported in reference 1 dealt with the effects of changes in leading-edge radius, Reynolds number, and Mach number on the longitudinal stability characteristics of 45° sweptback wings of aspect ratios of 3 and 5 and symmetrical 9-percent-thick airfoil sections. The present tests were made to determine the effects of a change of leading-edge radius on the longitudinal stability characteristics of several cambered wings which had the same plan form as those utilized in the tests of reference 1. Some data of reference 1, therefore, have been included to show the influence of camber. Only a brief discussion of the data is contained in the present report in order to expedite the release of these data.

The results of tests of the cambered wings were obtained through a range of tunnel air speeds at tunnel stagnation pressures of 14.7 and 33 pounds per square inch absolute. This permitted ranges of Reynolds number from 1.14×10^6 to 5.50×10^6 and from 1.80×10^6 to 8.00×10^6 with corresponding ranges of Mach number from 0.058 to 0.290 and from 0.024 to 0.204, respectively.

SYMBOLS

C_L lift coefficient, Lift/qS

C_{l_i} section design lift coefficient

C_m pitching-moment coefficient about $0.25\bar{c}$, Pitching moment/$qS\bar{c}$

S wing area, sq ft

$\bar{c}$ mean aerodynamic chord, $\frac{2}{S}\int_0^{b/2} c^2 dy$, ft

c local wing chord parallel to plane of symmetry, ft

y spanwise ordinate normal to plane of symmetry, ft

b wing span, ft

q	free-stream dynamic pressure, $\frac{1}{2}\rho V^2$, lb/sq ft
ρ	density of air, slugs/cu ft
V	free-stream velocity, ft/sec
R	Reynolds number
M	Mach number
$\Lambda_{c/4}$	sweepback of quarter-chord line
A	aspect ratio, b^2/S

MODEL

Four wings, the principal dimensions of which are given in figure 1, were used in the present tests. The geometric characteristics of these wings are as follows:

$\Lambda_{c/4}$, deg	Aspect ratio	Taper ratio	L.E. radius	Basic thickness form	Maximum camber
45	5	0.286	0.0089c	NACA 009-63	0.0245c
45	3	.500	.0089c	NACA 0009-63	.0245c
45	5	.286	.0025c	NACA 0009-(3.18)3	.0245c
45	3	.500	.0025c	NACA 0009-(3.18)3	.0245c

The thickness distribution of a modified NACA four-digit series airfoil was utilized since a systematic procedure for varying the leading-edge radius existed (ref. 2). An NACA 230 mean line modified for a design lift coefficient of 0.4 was combined with the thickness distribution. The changes in leading-edge radius of these airfoils resulted in changes of the section ordinates forward of the maximum thickness (30 percent chord). It may be noted from the foregoing table that taper ratio and aspect ratio change concurrently.

TESTS AND CORRECTIONS

The wings were supported in the tunnel by a system of normal supports which consisted of a pair of main struts and a pair of auxiliary struts. The tests were conducted through a range of air speeds at stagnation pressures of 14.7 and 33 pounds per square inch absolute. These pressure permitted ranges of Reynolds number and Mach number as follows:

Tunnel pressure, lb/sq in.	R		M	
	A = 5	A = 3	A = 5	A = 3
14.7	1.14×10^6 to 5.28×10^6	1.60×10^6 to 5.50×10^6	0.058 to 0.290	0.078 to 0.240
33	1.80×10^6 to 8.00×10^6	2.17×10^6 to 7.90×10^6	0.024 to 0.204	0.048 to 0.185

The pitching-moment coefficients and values of angle of attack have been corrected for jet-boundary effects by the method of reference 3. Inasmuch as the variations of lift and pitching-moment characteristics are of primary interest rather than the absolute values, tests to determine model support tare and interference effects were not conducted. A correction for the combined effect of model asymmetry, model support tare, and interference effects assumed for umcambered wing data presented in reference 1 have been applied to these data. The values of angle of attack have been corrected for 0.1° misalinement of the air stream based on results of previous tests in the Langley 19-foot pressure tunnel.

RESULTS AND DISCUSSION

The lift and pitching-moment characteristics obtained for the cambered wings of aspect ratios 3 and 5, having leading-edge radii of 0.89 and 0.25 percent chord are presented in figures 2 to 9. Figures 10 to 17 show the effects of a change in leading-edge radius, the effect of camber, and the effects of Reynolds number and Mach number on the longitudinal stability characteristics of these wings.

Effect of a Change of Leading-Edge Radius

The pitching-moment characteristics presented in figures 10 and 11 indicate that decrease in leading-edge radius of the aspect-ratio-3 and 5 wings from 0.89 to 0.25 percent chord resulted mainly in a decrease in the lift coefficients beyond which destabilizing changes associated with wing-tip stall, occurred. For example, the decrease in leading-edge radius of the aspect-ratio-3 wing resulted in a decrease of approximately 0.20 in the lift coefficient beyond which destabilizing changes occur, as compared to an incremental change in lift coefficient of approximately 0.10 for the aspect-ratio-5 wing. The aspect-ratio-5 wing, having 0.25-percent chord leading-edge radius, and the aspect-ratio-3 wing, having either 0.25- or 0.89-percent chord leading-edge radius exhibited stabilizing changes of varying degrees at a lift coefficient prior to the destabilizing changes. Visual studies of the flow appeared to indicate that flow changes occurred concurrently with these stabilizing changes along the leading edge of the outboard sections. It may be noted from figure 10 that variation in the lift coefficients for the stabilizing changes resulting from a change in leading-edge radius of the aspect-ratio-3 wing were noticeably smaller than the corresponding lift coefficient variations of the destabilizing changes.

Effect of Camber

The effect of camber as shown by several comparisons of the cambered and uncambered (ref. 1) wings (figs. 12 and 13) indicates that the addition of camber to wings of both aspect ratios resulted mainly in an increase in the lift coefficient at which destabilizing changes associated with tip stall occurred. These changes were somewhat greater at low Reynolds numbers than at high Reynolds numbers for the aspect-ratio-3 wing (fig. 12). It may be noted in figure 13 that the effect of camber on the aspect-ratio-5 wing is appreciably larger for the smaller leading-edge radius.

Effects of Reynolds Number and Mach Number

The data presented in figures 14 to 17 give some indication as to the interrelated effects of Reynolds number and Mach number on the longitudinal stability characteristics of the various cambered wings tested. In general, an increase in Reynolds number at a constant Mach number delayed the stability changes associated with flow separation for the wings of both aspect ratios. Similar effects of Reynolds number were noted in reference 1 for wings having symmetrical airfoil sections.

For a given Reynolds number, an increase in Mach number resulted in a decrease in the lift coefficient at which destabilizing changes in the

pitching-moment characteristics of the aspect-ratio-3 wing occurred. It may be noted in figure 16 that at a Reynolds number of 5.0×10^6, the lift coefficient at which destabilizing changes occurred with the aspect-ratio-3 wing having 0.89-percent-chord leading-edge radius decreased from approximately 1.2 to 1.1 with increase in Mach number from approximately 0.10 to 0.24. Decrease in leading-edge radius resulted in an appreciable decrease in the effects of Mach number on the aspect-ratio-3 wing. The effects of Mach number on the aspect-ratio-5 wing were negligible. The Mach number effects found in reference 1 were appreciably larger than those found for the present cambered wings.

CONCLUDING REMARKS

In general, an increase in leading-edge radius from 0.25 to 0.89 percent chord, the addition of camber, or an increase in Reynolds number for a constant Mach number resulted mainly in a delay to a higher lift coefficient of marked destabilizing changes in the pitching-moment characteristics. An increase in Mach number for a Reynolds number of 5.00×10^6 resulted in a decrease in the lift coefficient at which destabilizing changes of the aspect-ratio-3 wing occurred, but had no appreciable effect on the stability characteristics of the aspect-ratio-5 wing. The Mach number effects were, on the whole, appreciably less than were found for uncambered wings.

Langley Aeronautical Laboratory,
National Advisory Committee for Aeronautics,
Langley Field, Va., July 27, 1955.

REFERENCES

1. Foster, Gerald V., and Schneider, William C.: Effects of Leading-Edge Radius on the Longitudinal Stability of Two 45° Sweptback Wings as Influenced by Reynolds Numbers up to 8.20×10^6 and Mach Numbers up to 0.303. NACA RM L55F06, 1955.

2. Stack, John, and Von Doenhoff, Albert E.: Tests of 16 Related Airfoils at High Speeds. NACA Rep. 492, 1934.

3. Sivells, James C., and Salmi, Rachel M.: Jet-Boundary Corrections for Complete and Semispan Swept Wings in Closed Circular Wind Tunnels. NACA TN 2454, 1951.

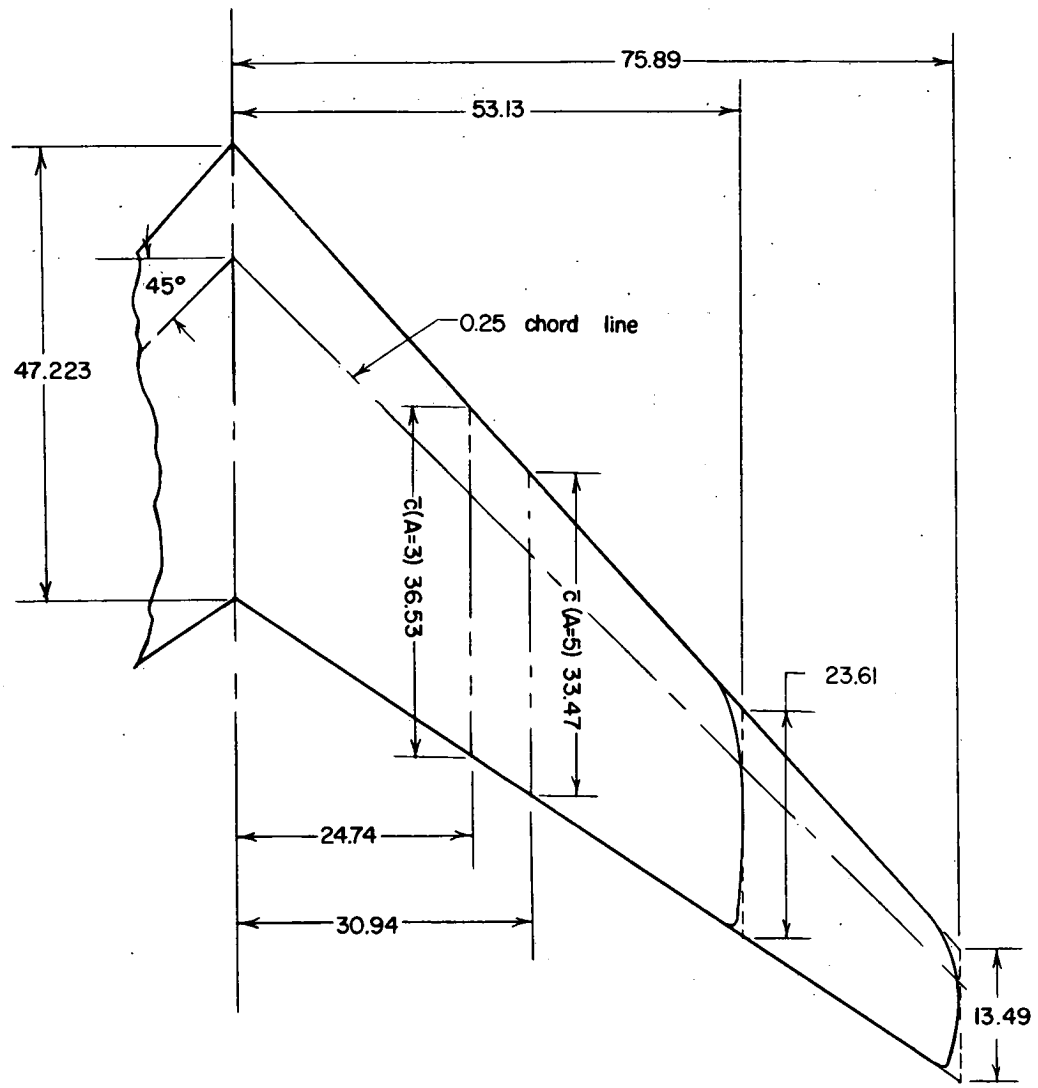

Figure 1.- Geometric details of the models. All dimensions are in inches unless otherwise noted.

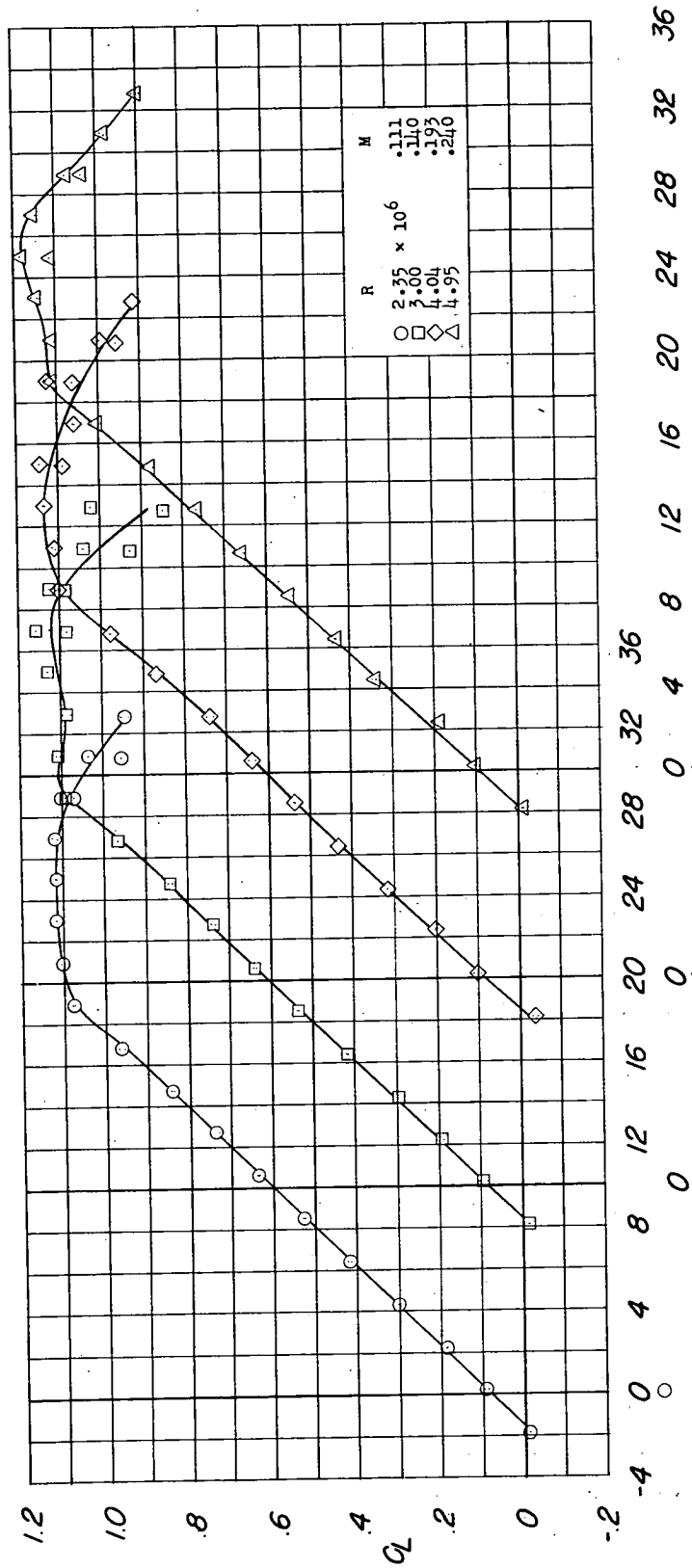

(a) C_L against α; atmospheric pressure.

Figure 2.- Variation of lift and pitching-moment coefficients with angle of attack of a 45° sweptback wing. Aspect ratio, 3; C_{l_i} = 0.4; leading-edge radius, 0.0089c.

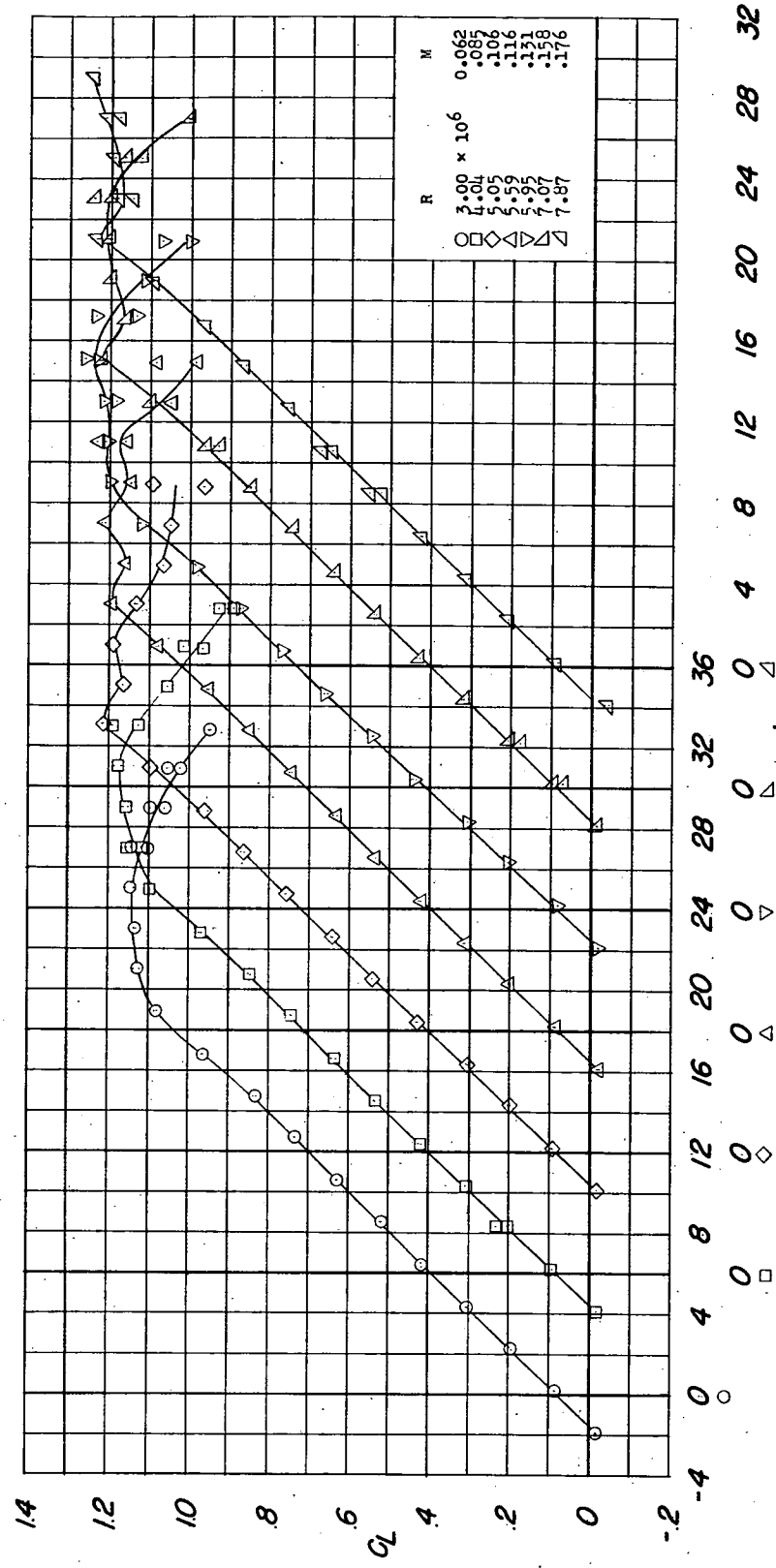

(b) C_L against α; pressure, 33 pounds per square inch.

Figure 2.- Continued.

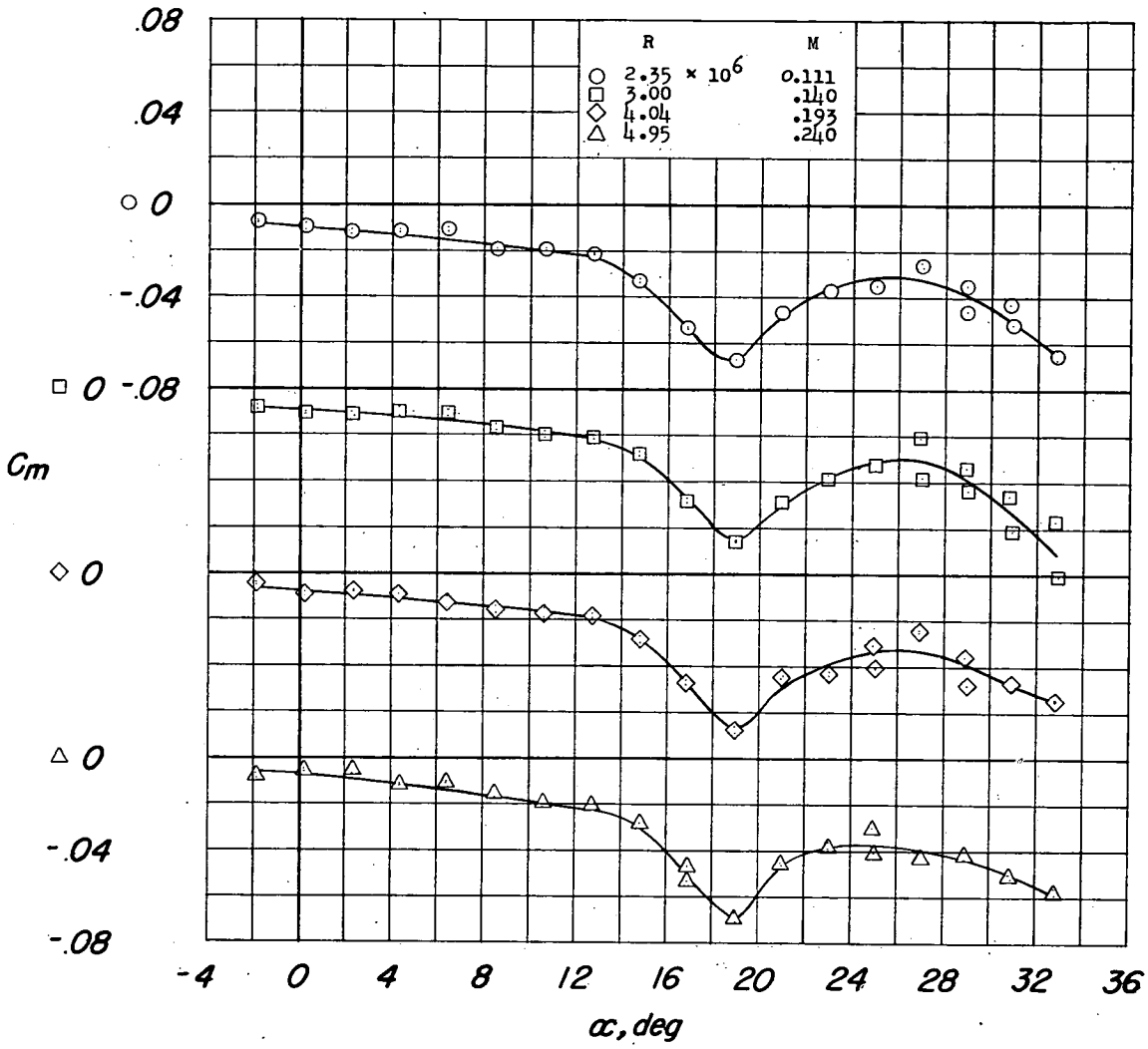

(c) C_m against α; atmospheric pressure.

Figure 2.- Continued.

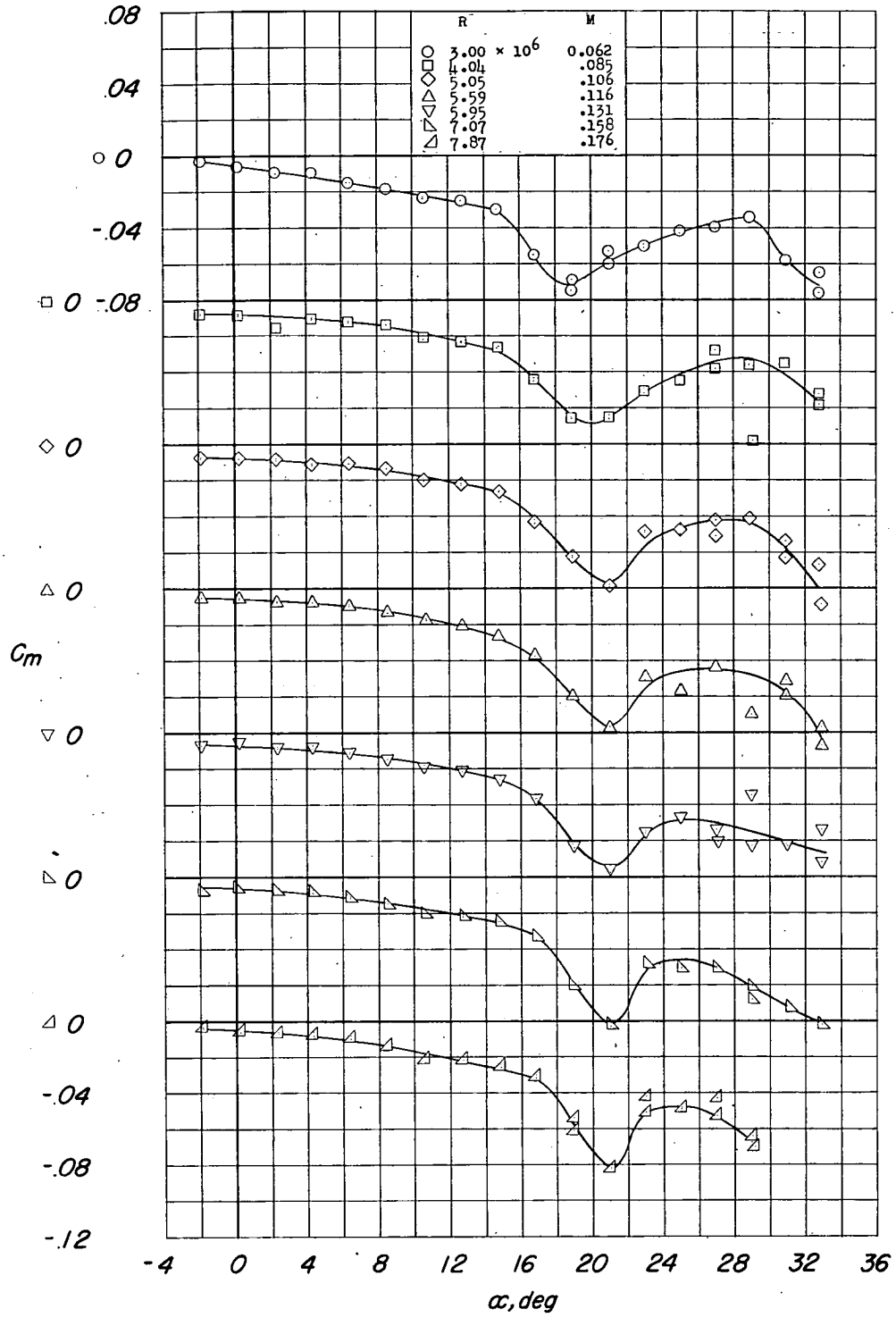

(d) C_m against α; pressure, 33 pounds per square inch.

Figure 2.- Concluded.

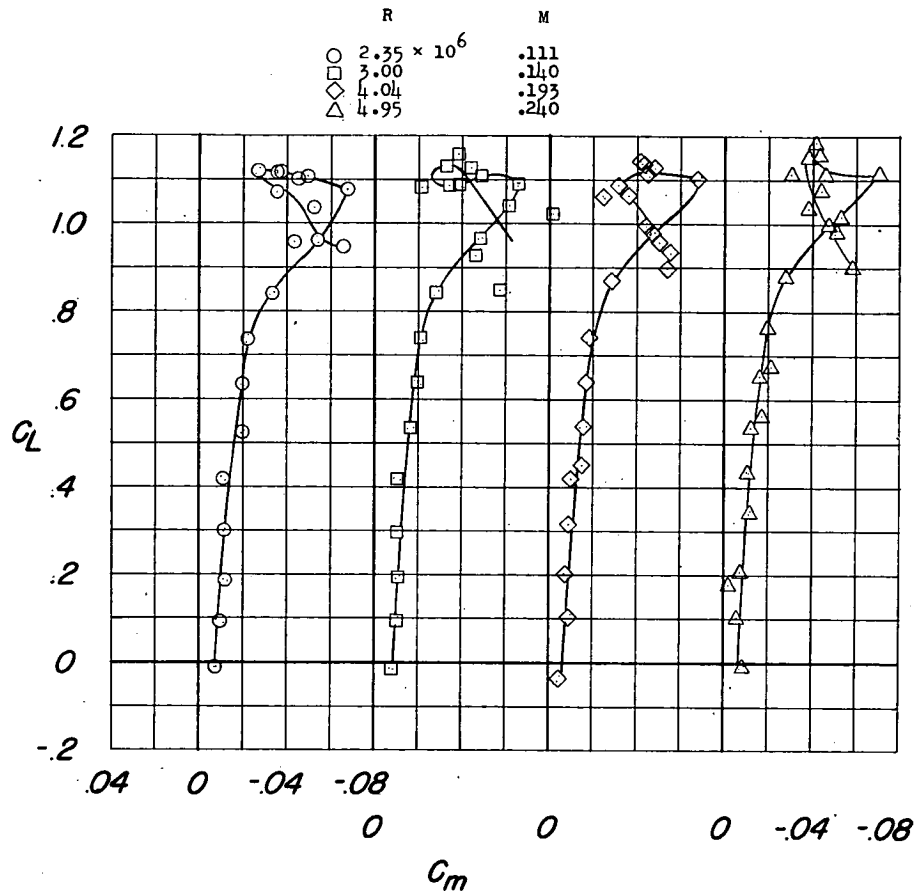

(a) Atmospheric pressure.

Figure 3.- Variation of pitching-moment coefficient with lift coefficient of a 45° sweptback wing. Aspect ratio, 3; $C_{l_i} = 0.4$; leading-edge radius, 0.0089c.

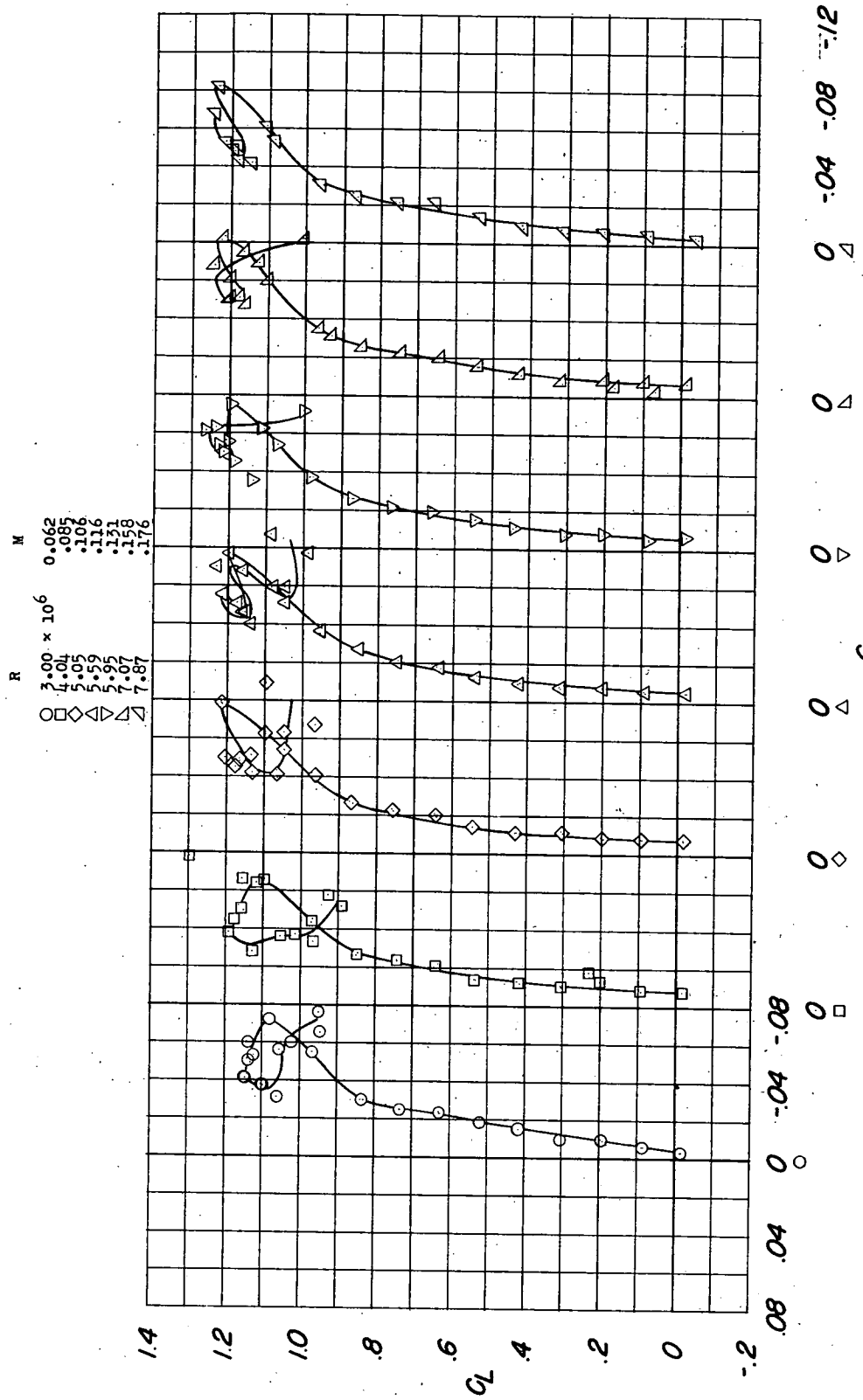

(b) Pressure, 33 pounds per square inch.

Figure 3.- Concluded.

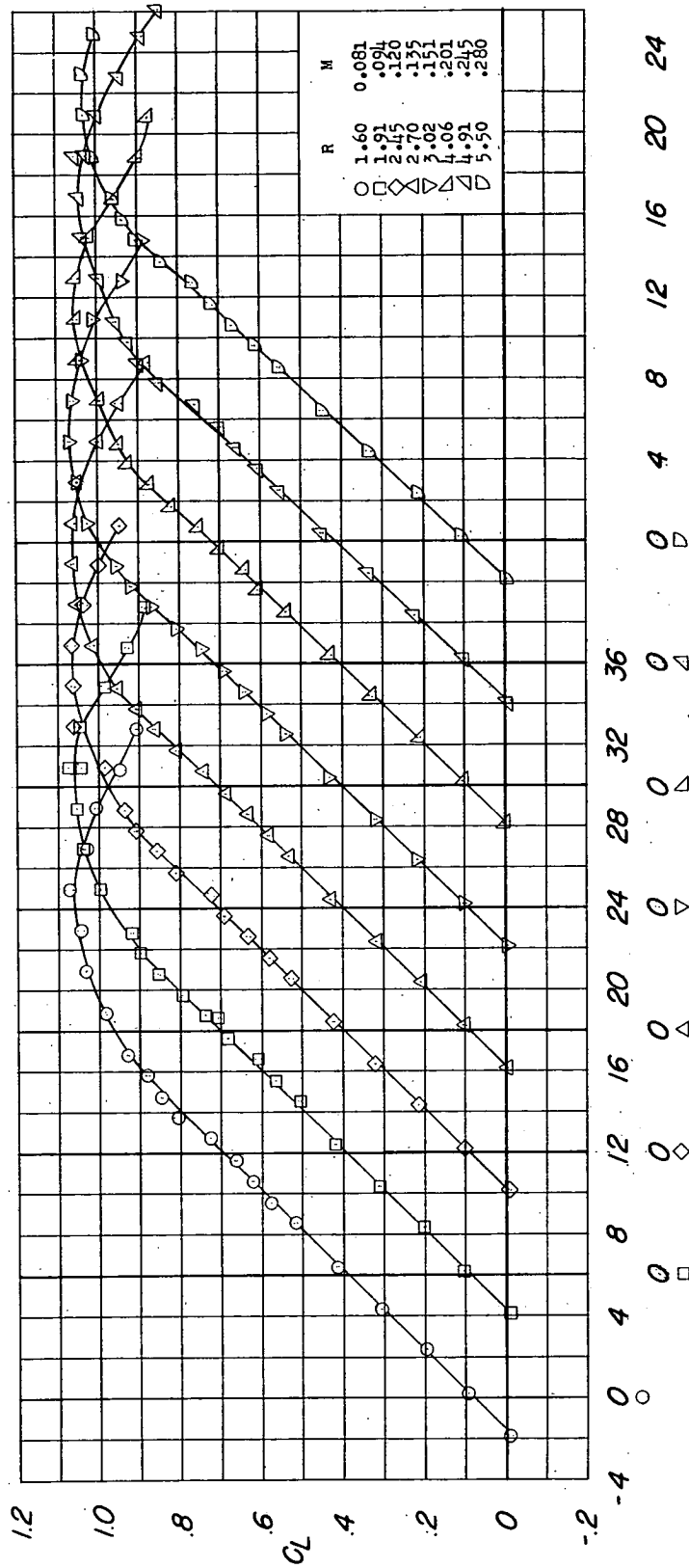

(a) C_L against α; atmospheric pressure.

Figure 4.- Variation of lift and pitching-moment coefficients with angle of attack of a 45° sweptback wing. Aspect ratio, 3; $C_{l_1} = 0.4$; leading-edge radius, 0.0025c.

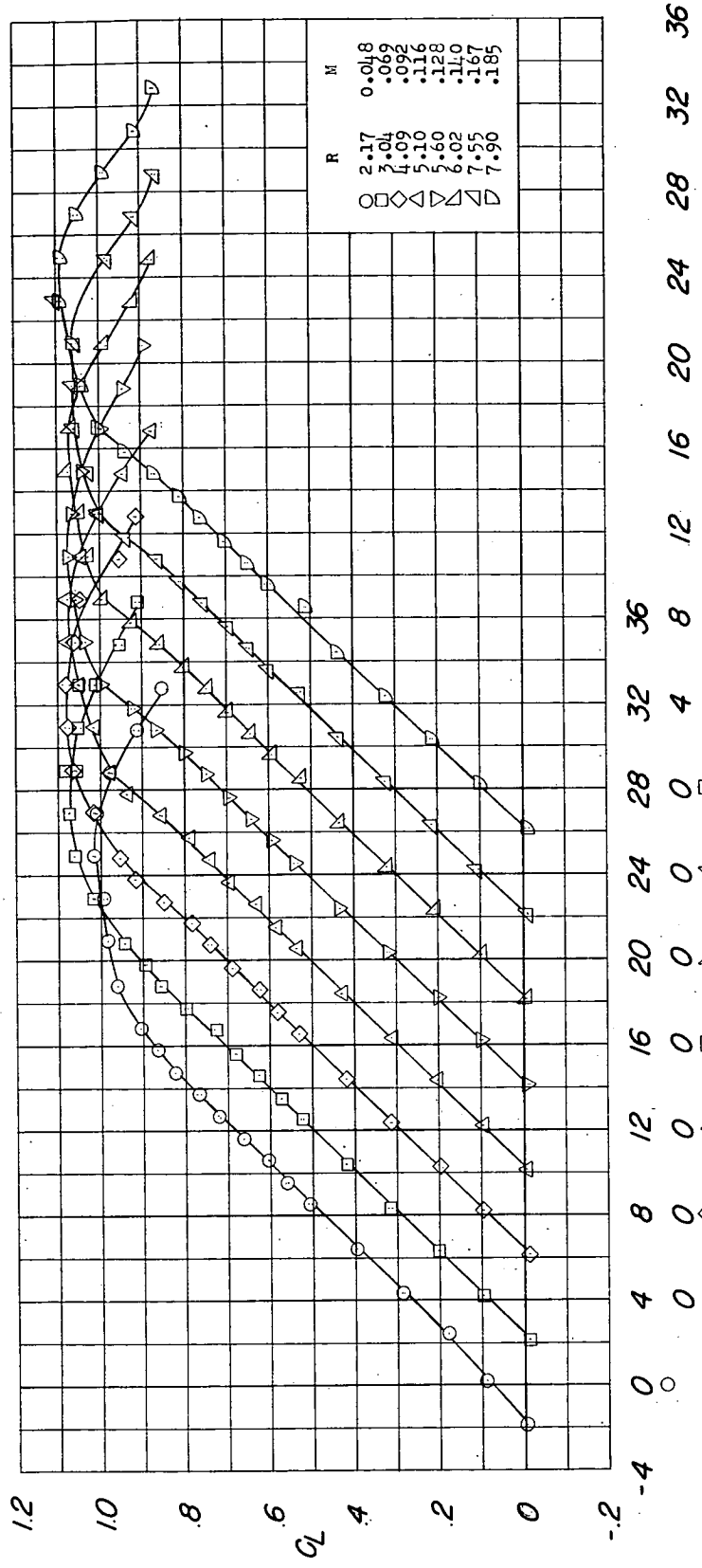

(b) C_L against α; pressure, 33 pounds per square inch.

Figure 4.- Continued.

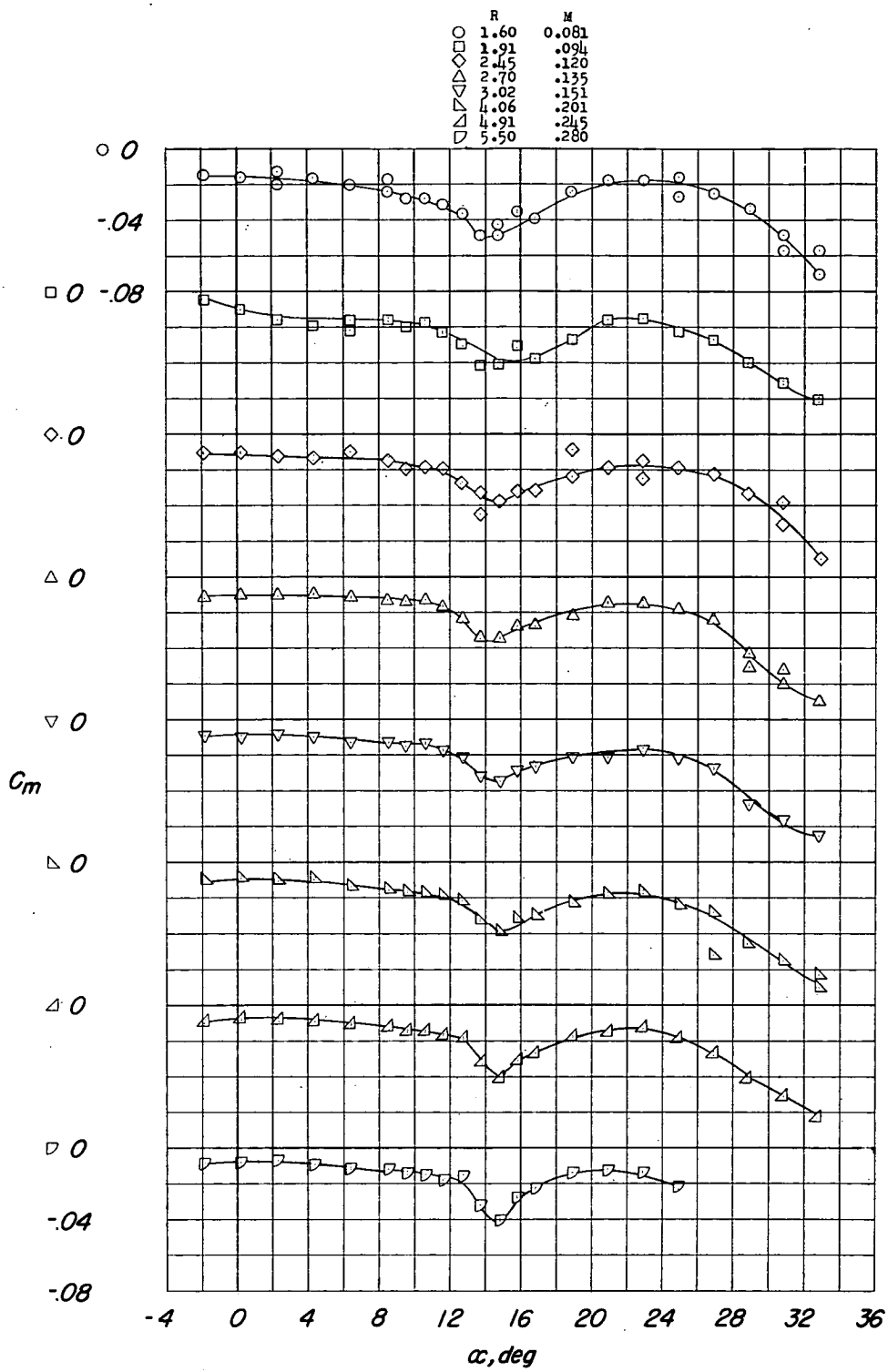

(c) C_m against α; atmospheric pressure.

Figure 4.- Continued.

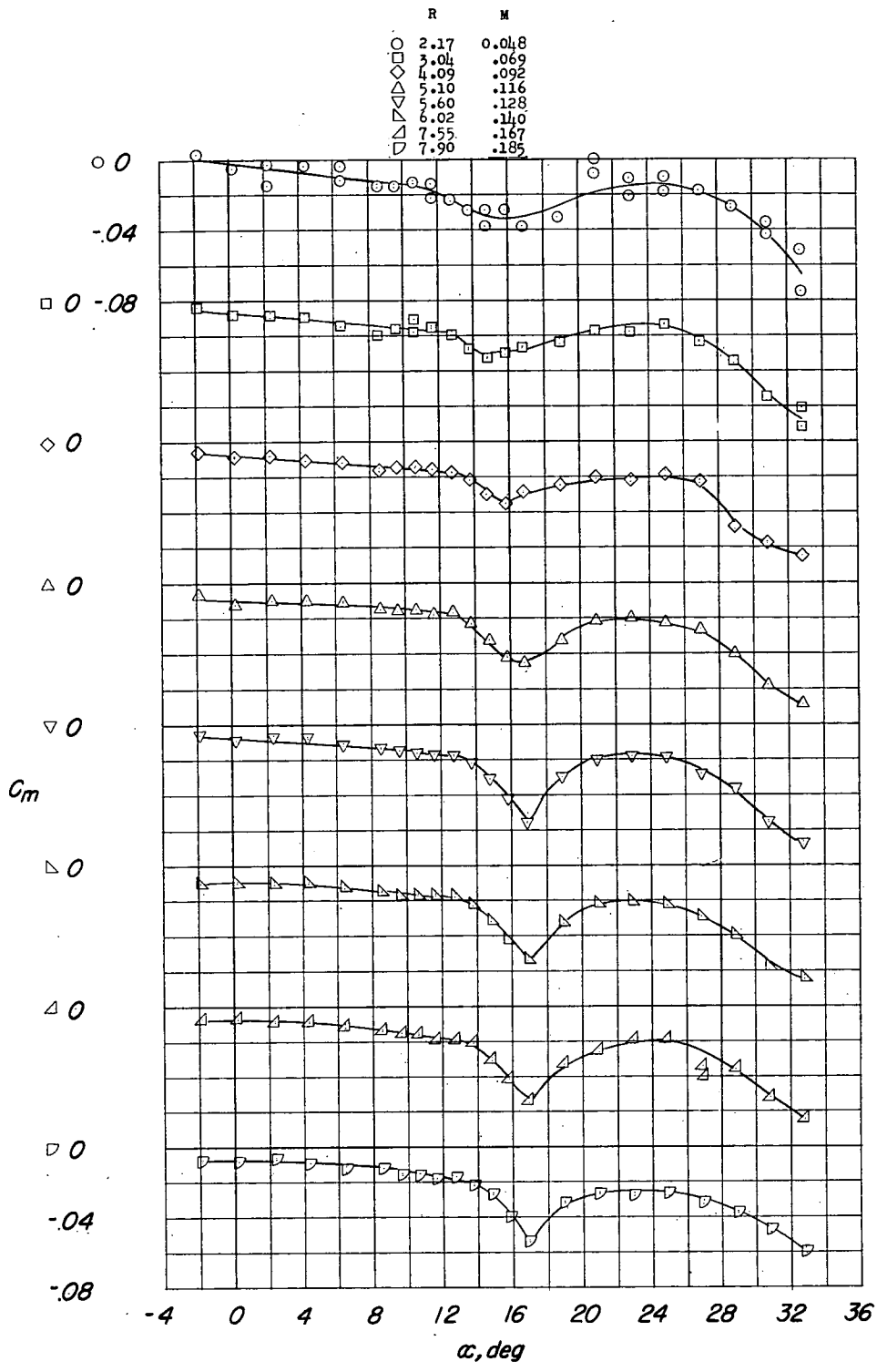

(d) C_m against α; pressure, 33 pounds per square inch.

Figure 4.- Concluded.

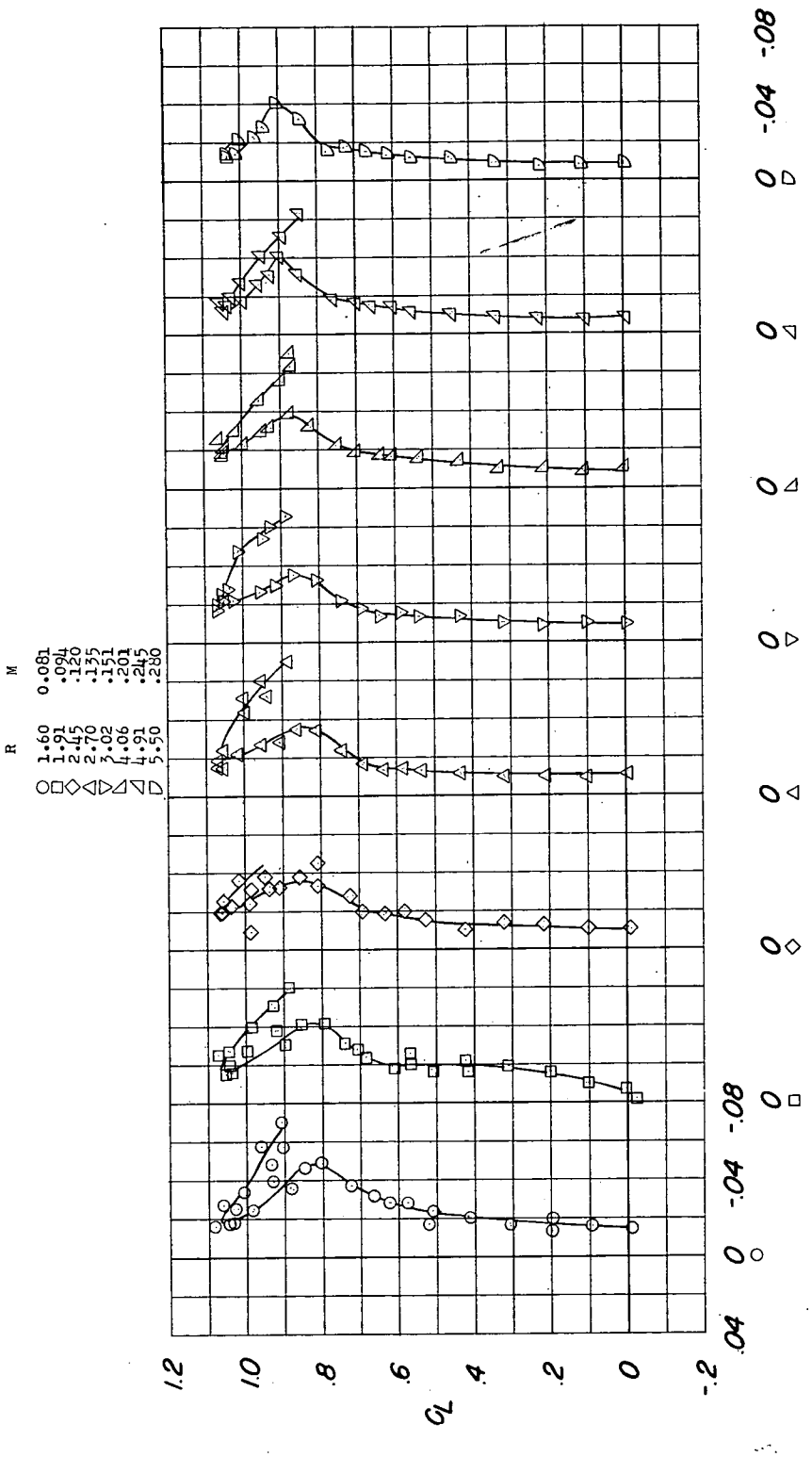

(a) Atmospheric pressure.

Figure 5.- Variation of pitching-moment coefficient with lift coefficient of a 45° sweptback wing. Aspect ratio, 3; $C_{l_i} = 0.4$; leading-edge radius, 0.0025c.

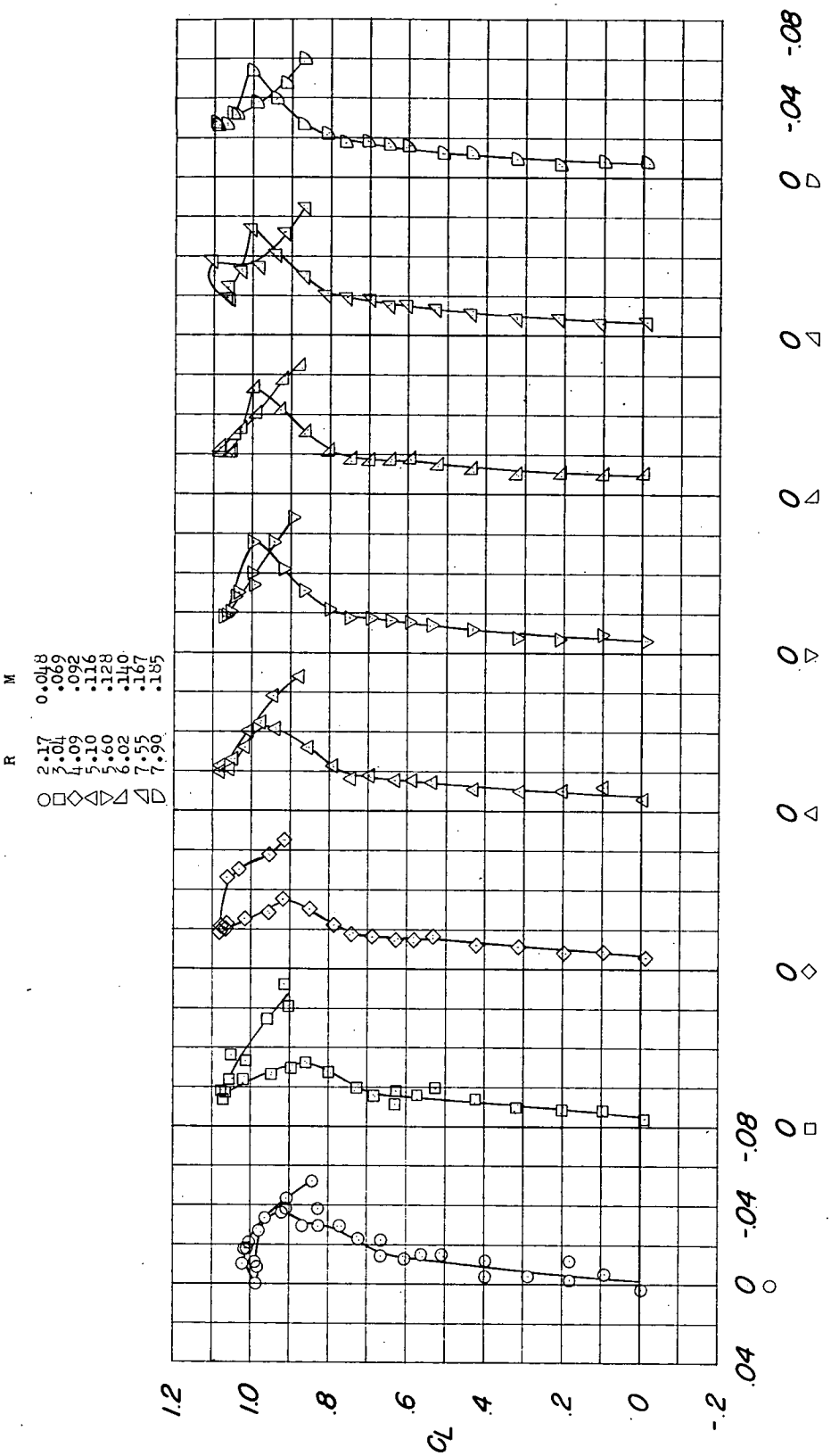

(b) Pressure, 33 pounds per square inch.

Figure 5.- Concluded.

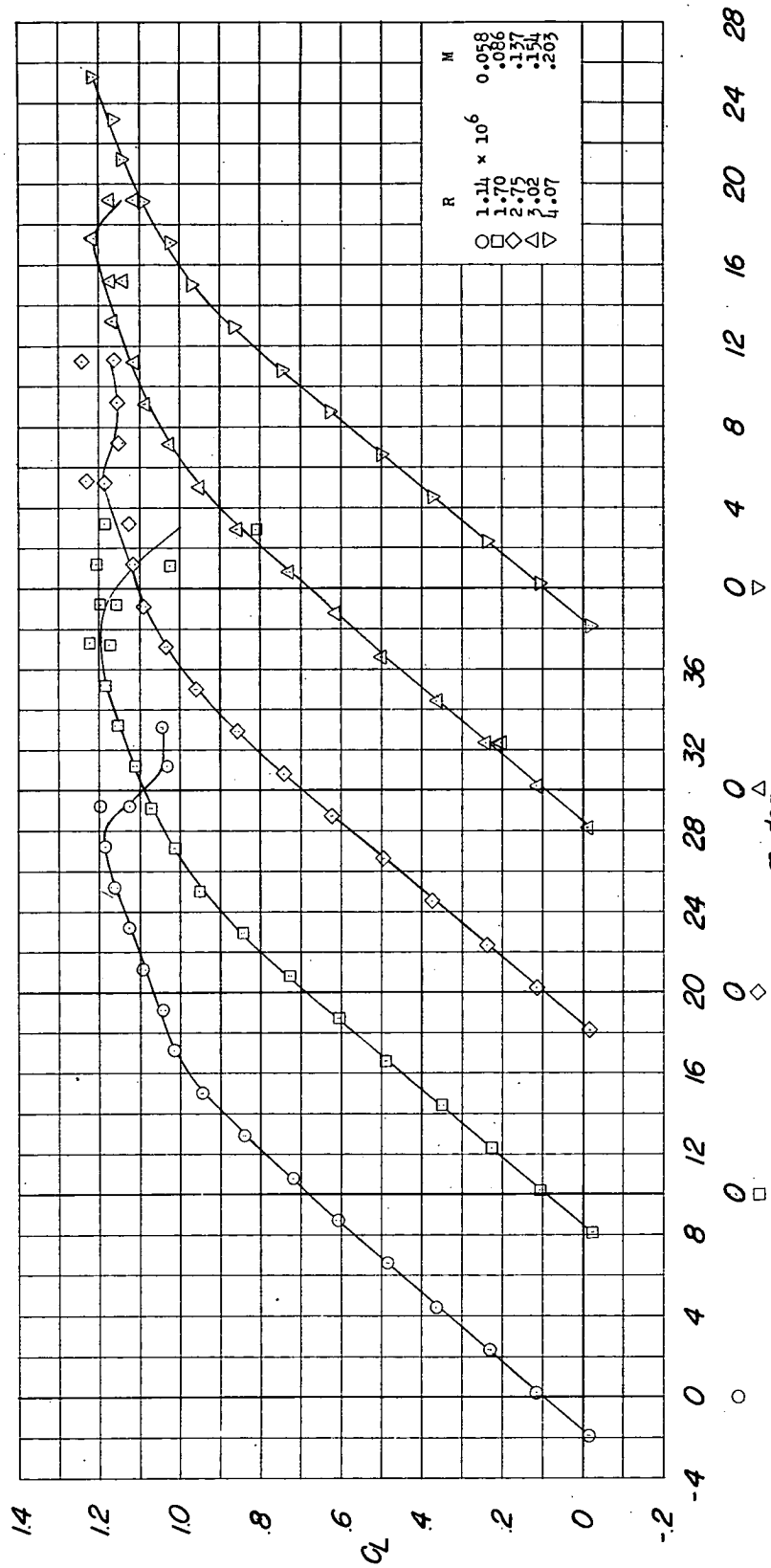

(a) C_L against α; atmospheric pressure.

Figure 6.- Variation of lift and pitching-moment coefficients with angle of attack of a 45° sweptback wing. Aspect ratio, 5; C_{l_i} = 0.4; leading-edge radius, 0.0089c.

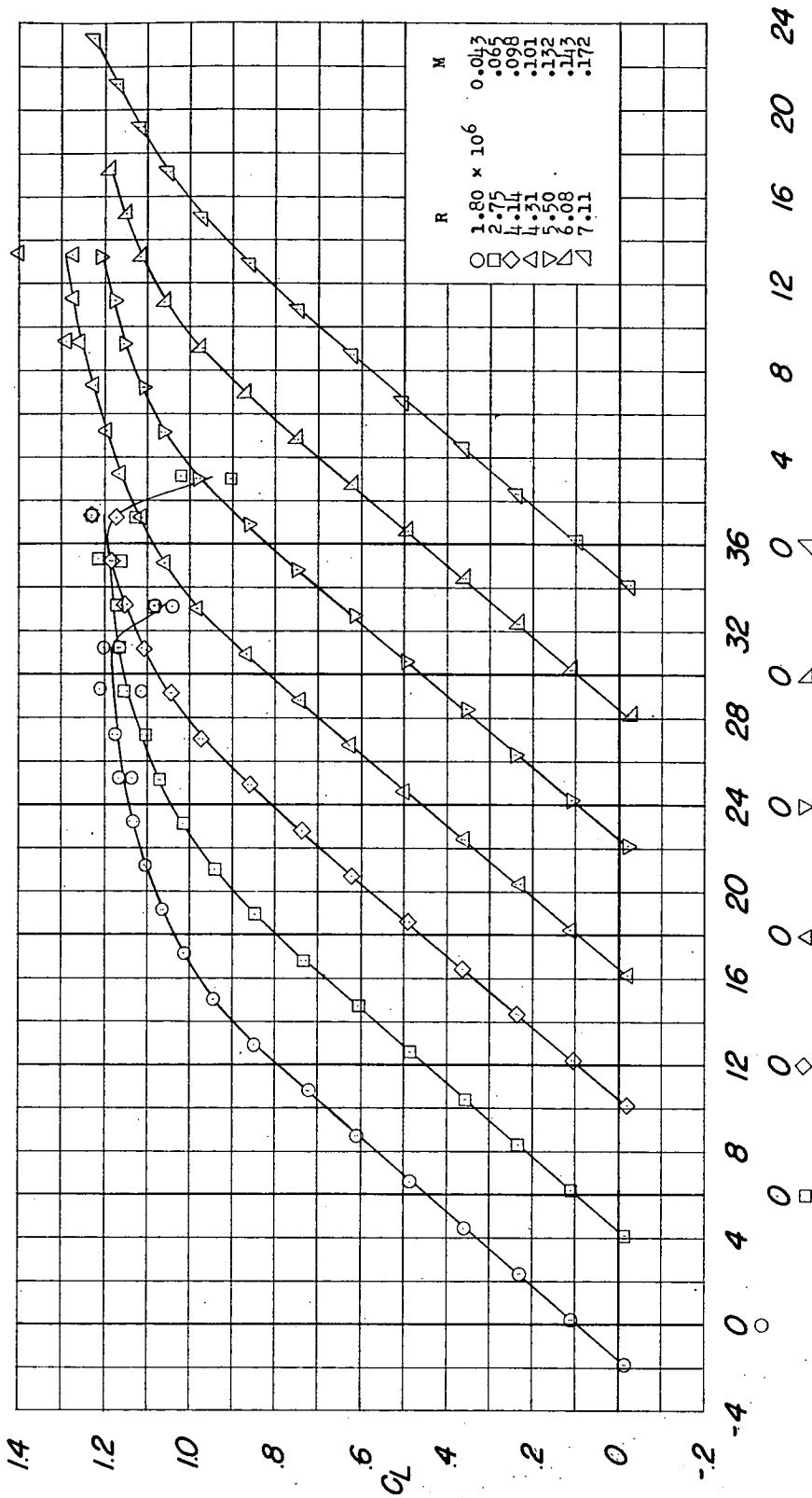

(b) C_L against α; pressure, 33 pounds per square inch.

Figure 6.- Continued.

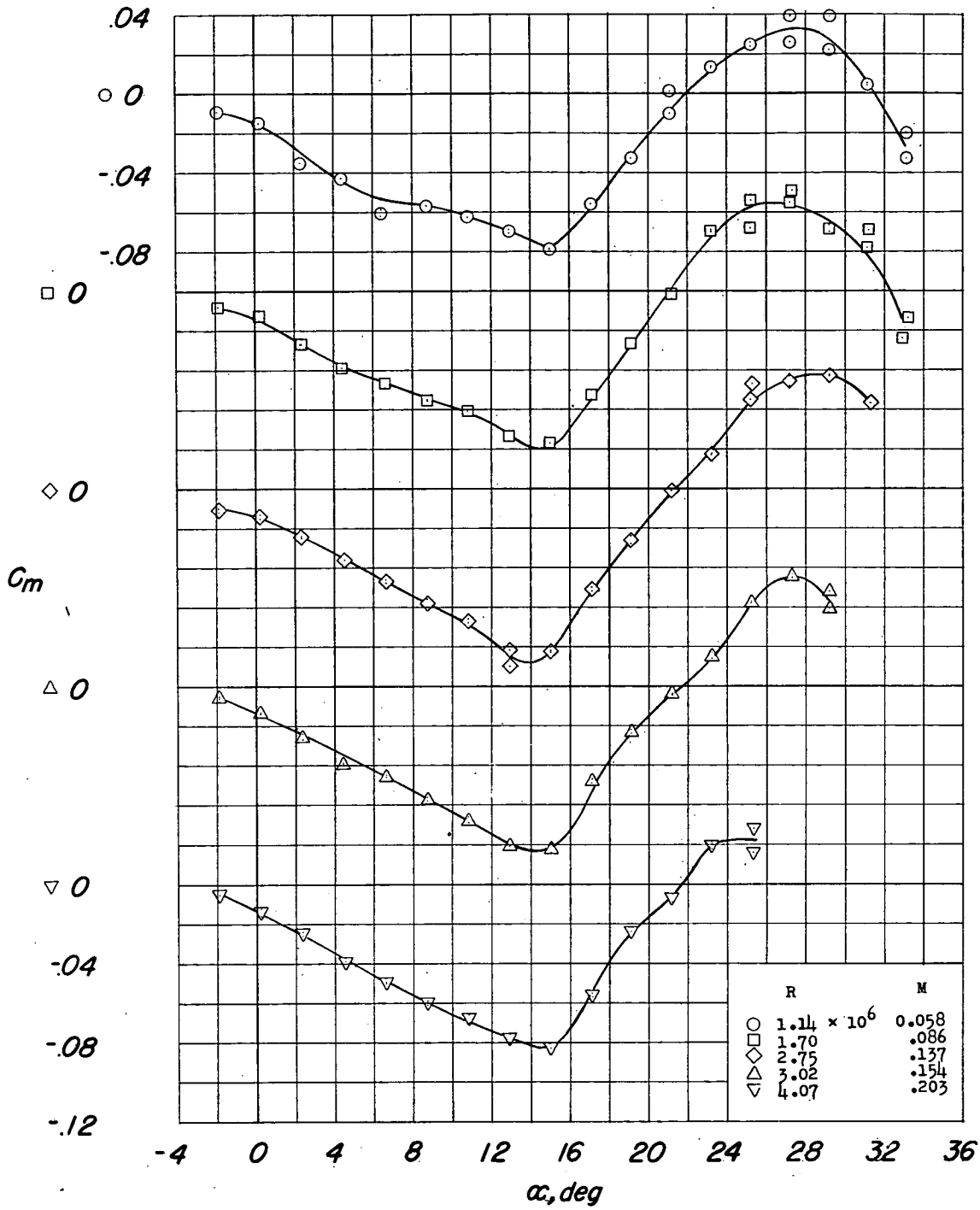

(c) C_m against α; atmospheric pressure.

Figure 6.- Continued.

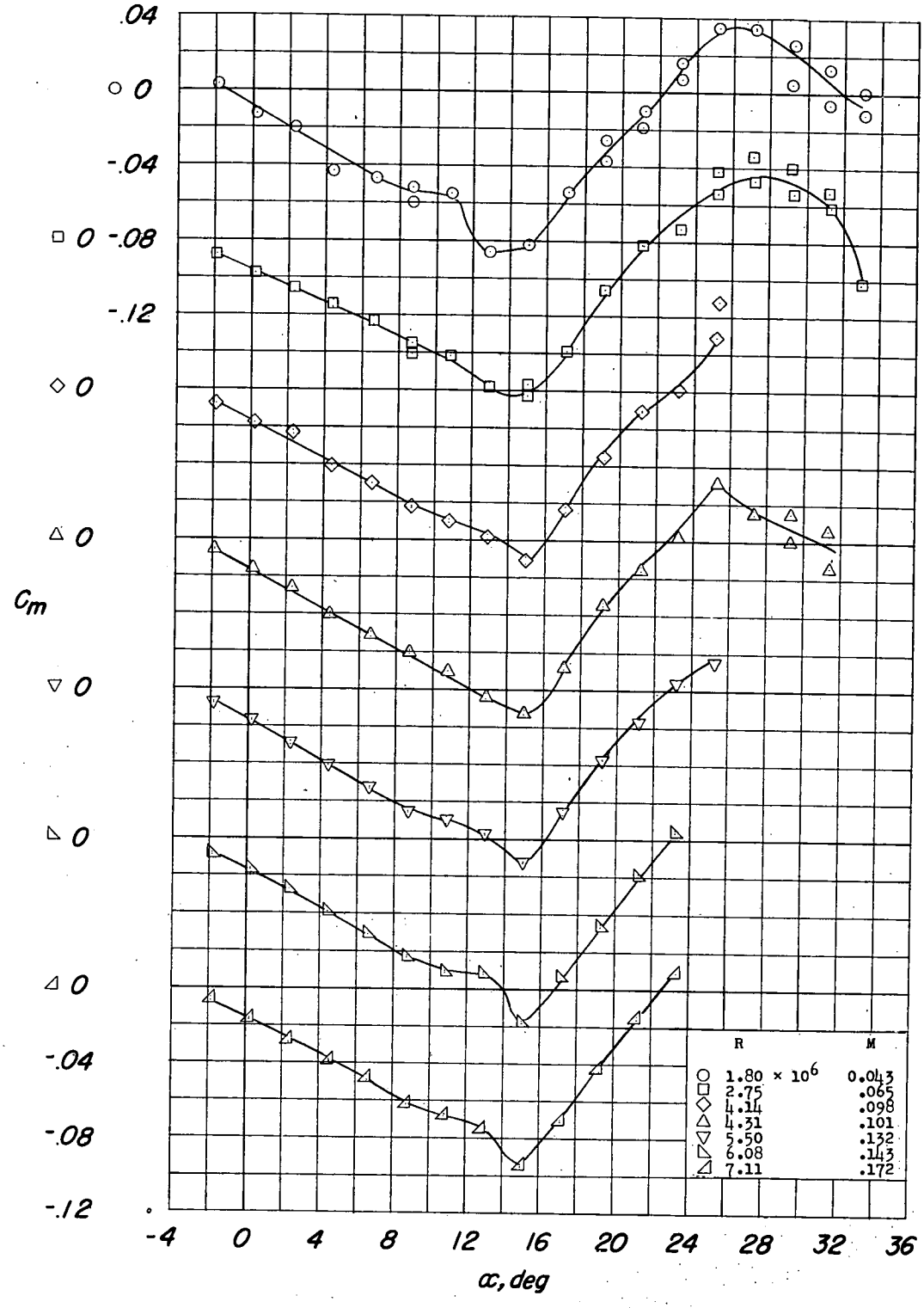

(d) C_m against α; pressure, 33 pounds per square inch.

Figure 6.- Concluded.

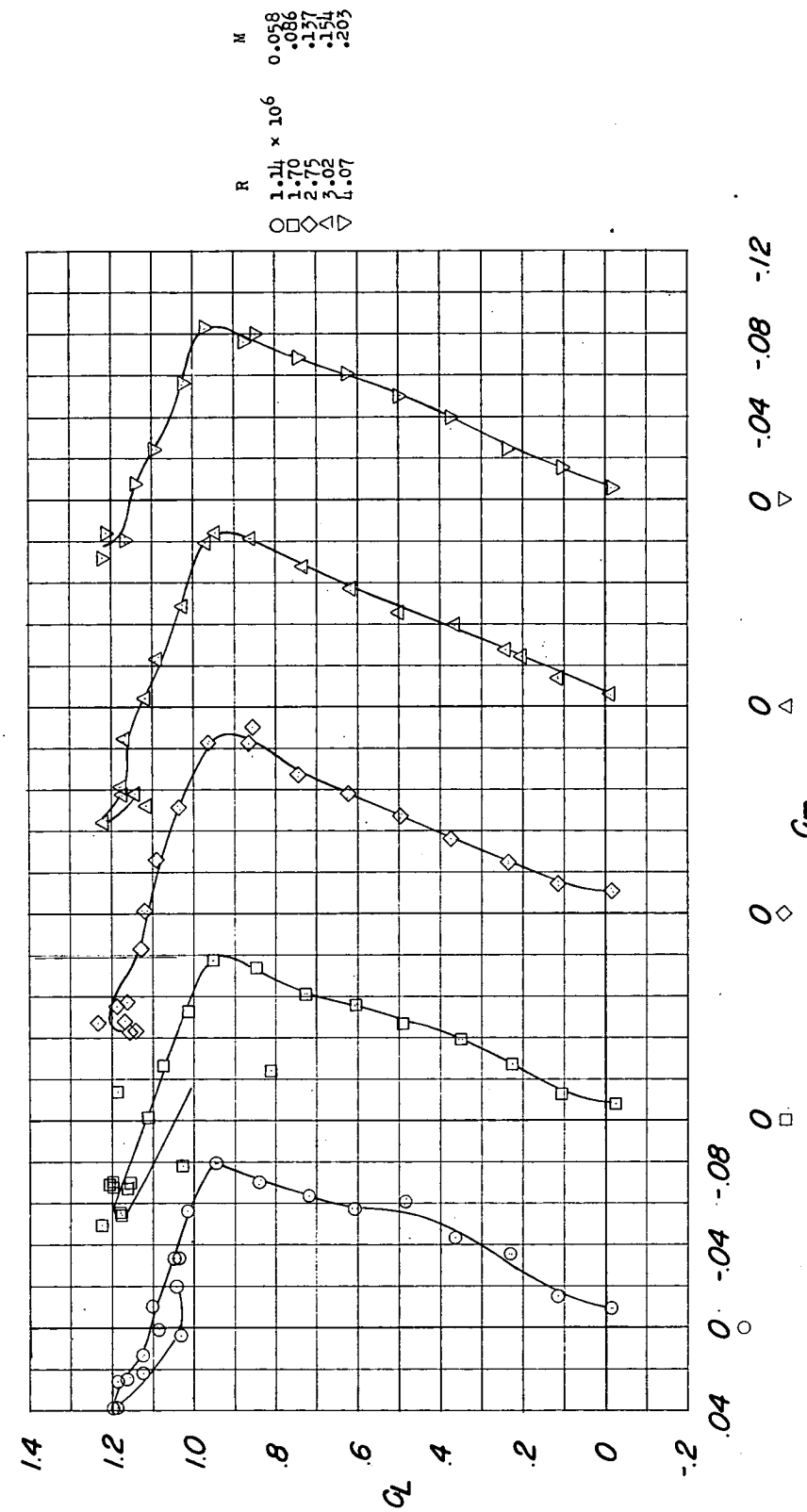

(a) Atmospheric pressure.

Figure 7.- Variation of pitching-moment coefficient with lift coefficient of a 45° sweptback wing. Aspect ratio, 5; C_{l_i} = 0.4; leading-edge radius, 0.0089c.

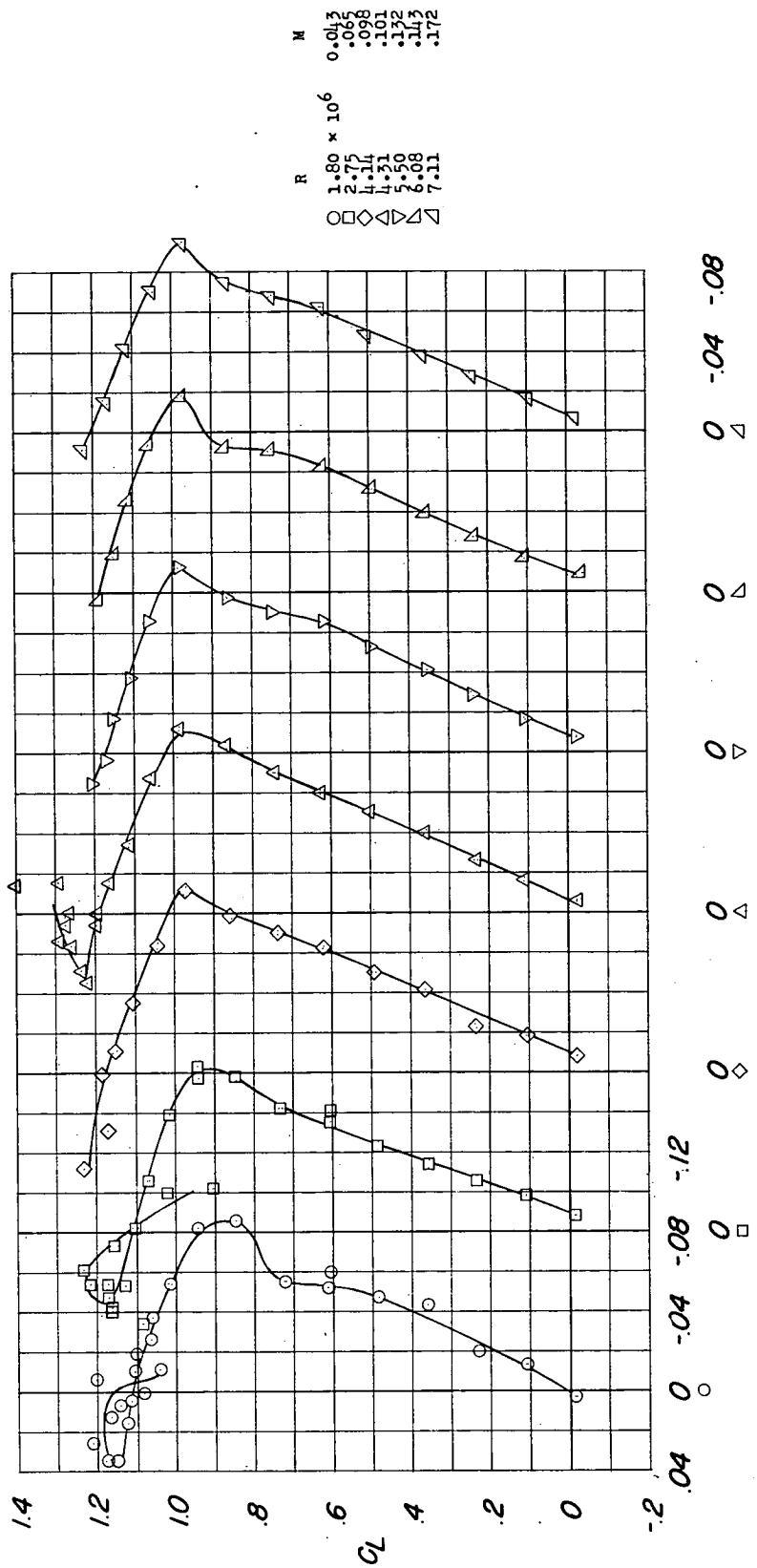

(b) Pressure, 33 pounds per square inch.

Figure 7.- Concluded.

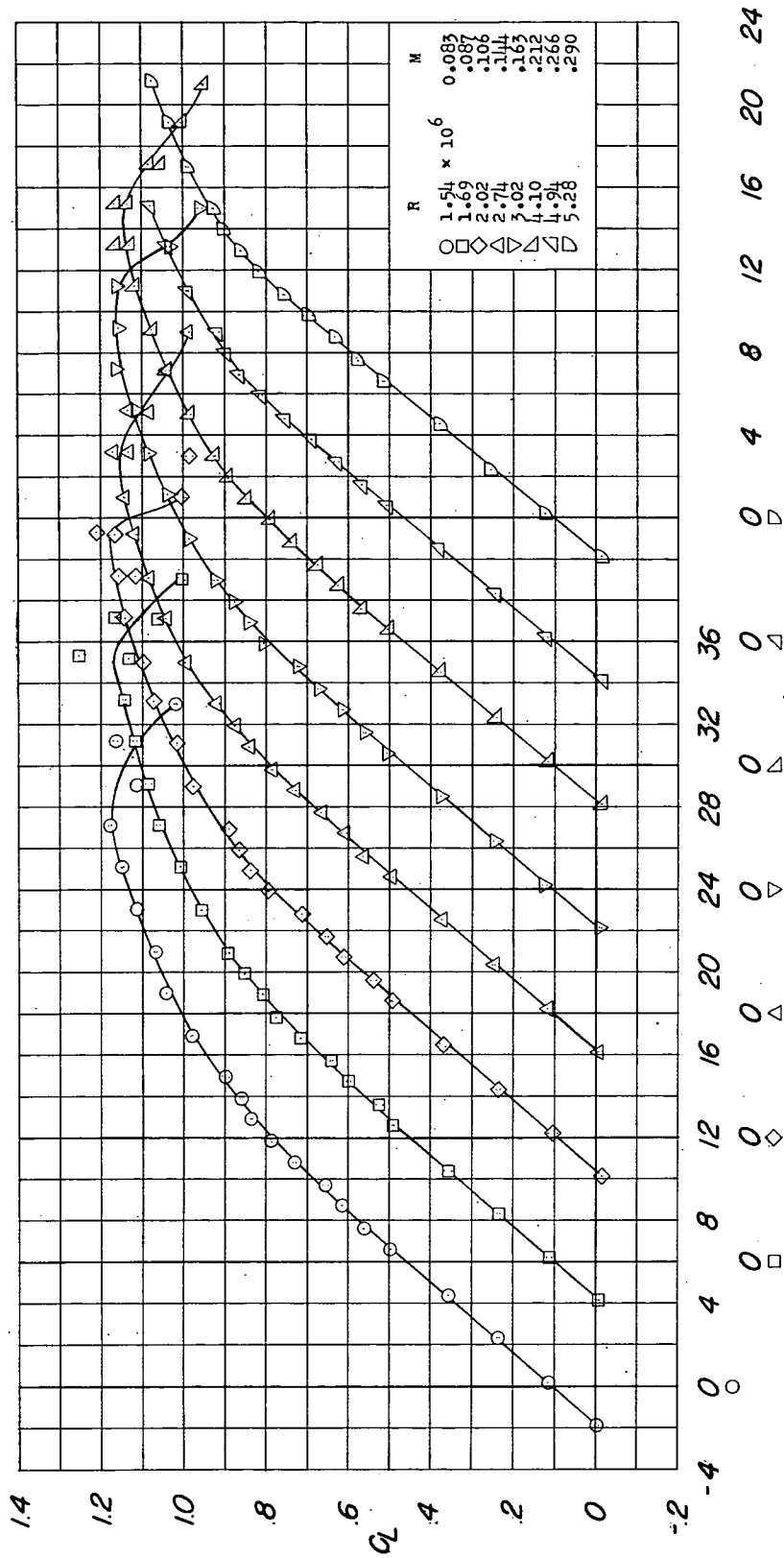

(a) C_L against α; atmospheric pressure.

Figure 8.- Variation of lift and pitching-moment coefficients with angle of attack of a 45° sweptback wing. Aspect ratio, 5; C_{l_i} = 0.4; leading-edge radius, 0.0025c.

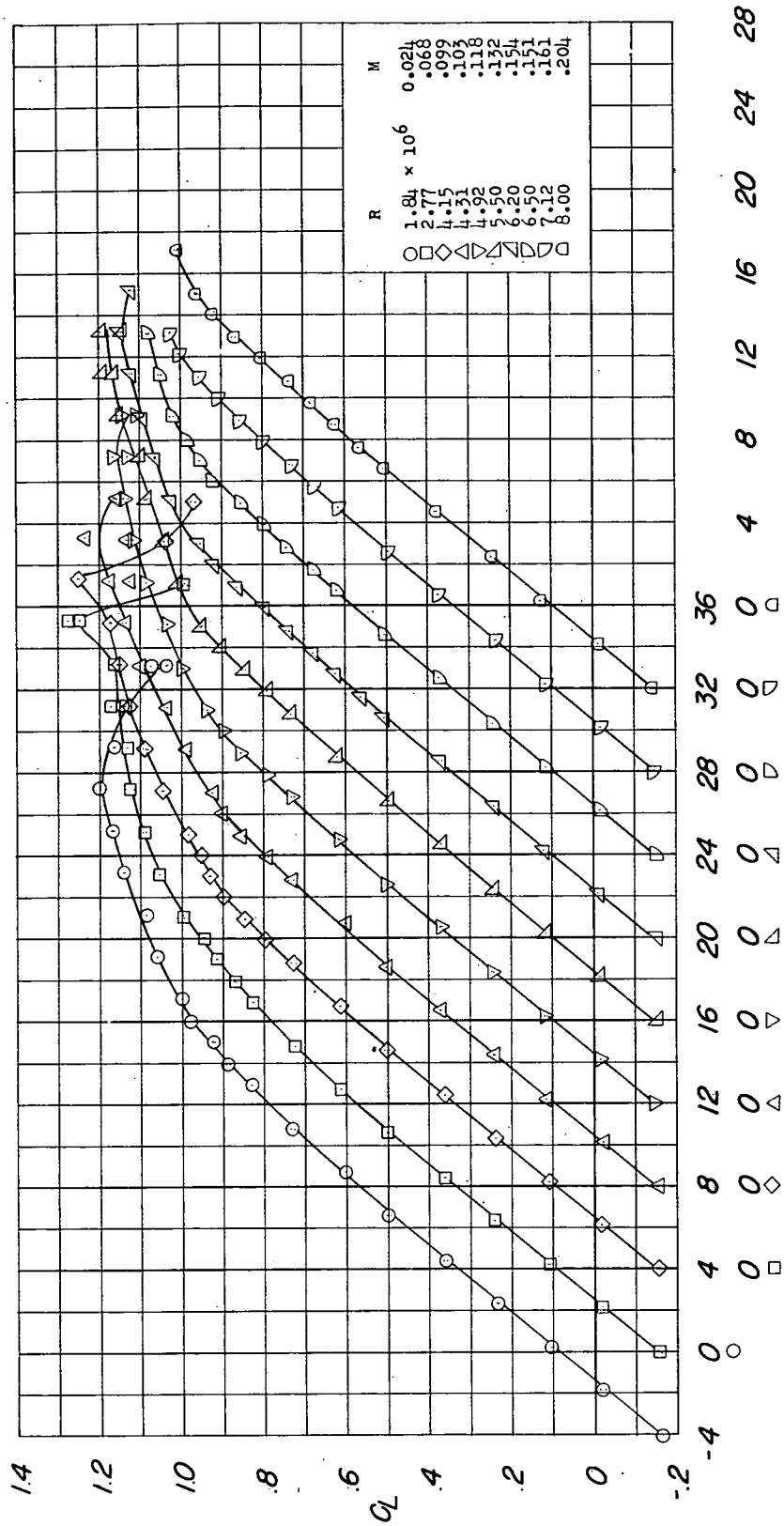

(b) C_L against α; pressure, 33 pounds per square inch.

Figure 8.- Continued.

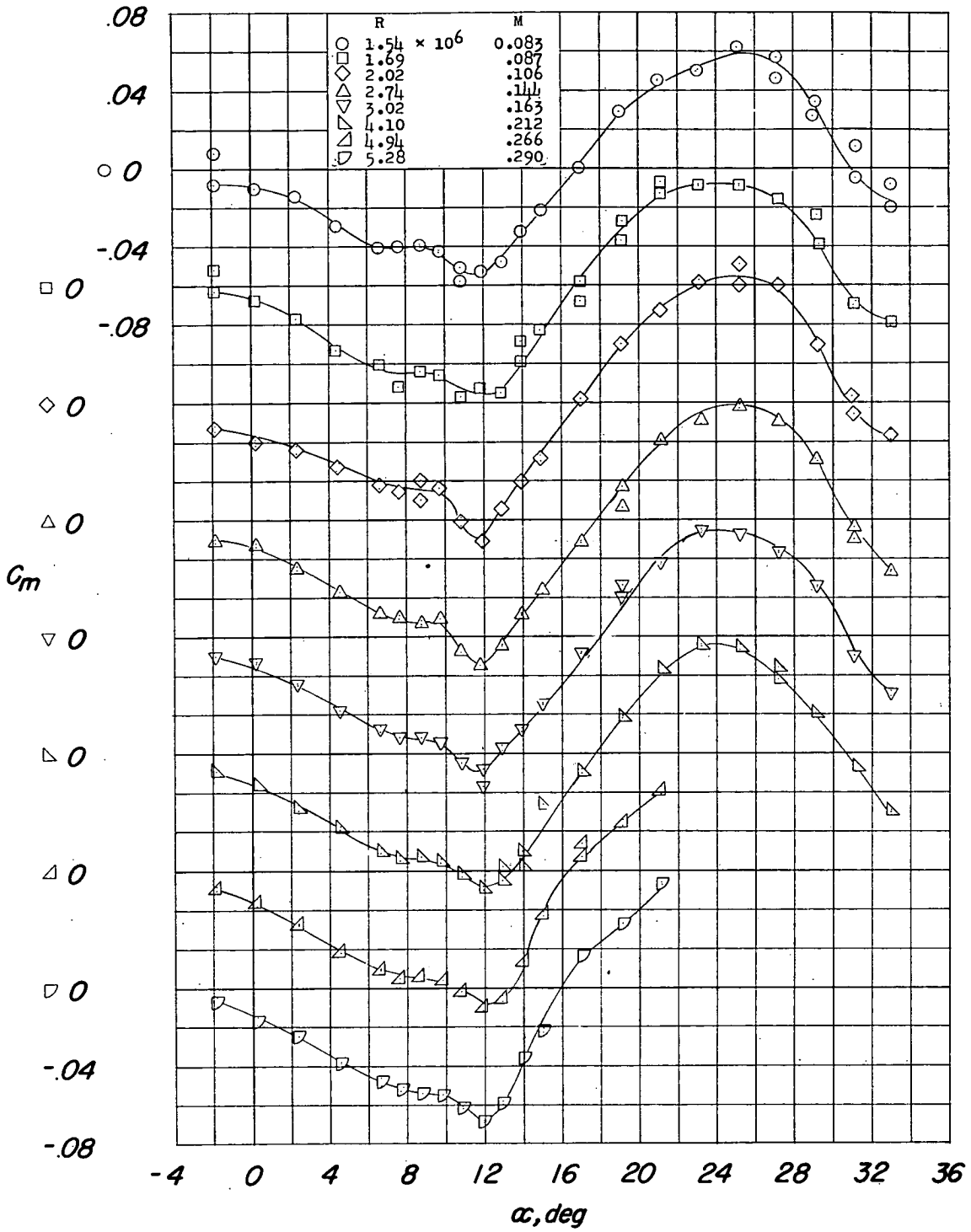

(c) C_m against α; atmospheric pressure.

Figure 8.- Continued.

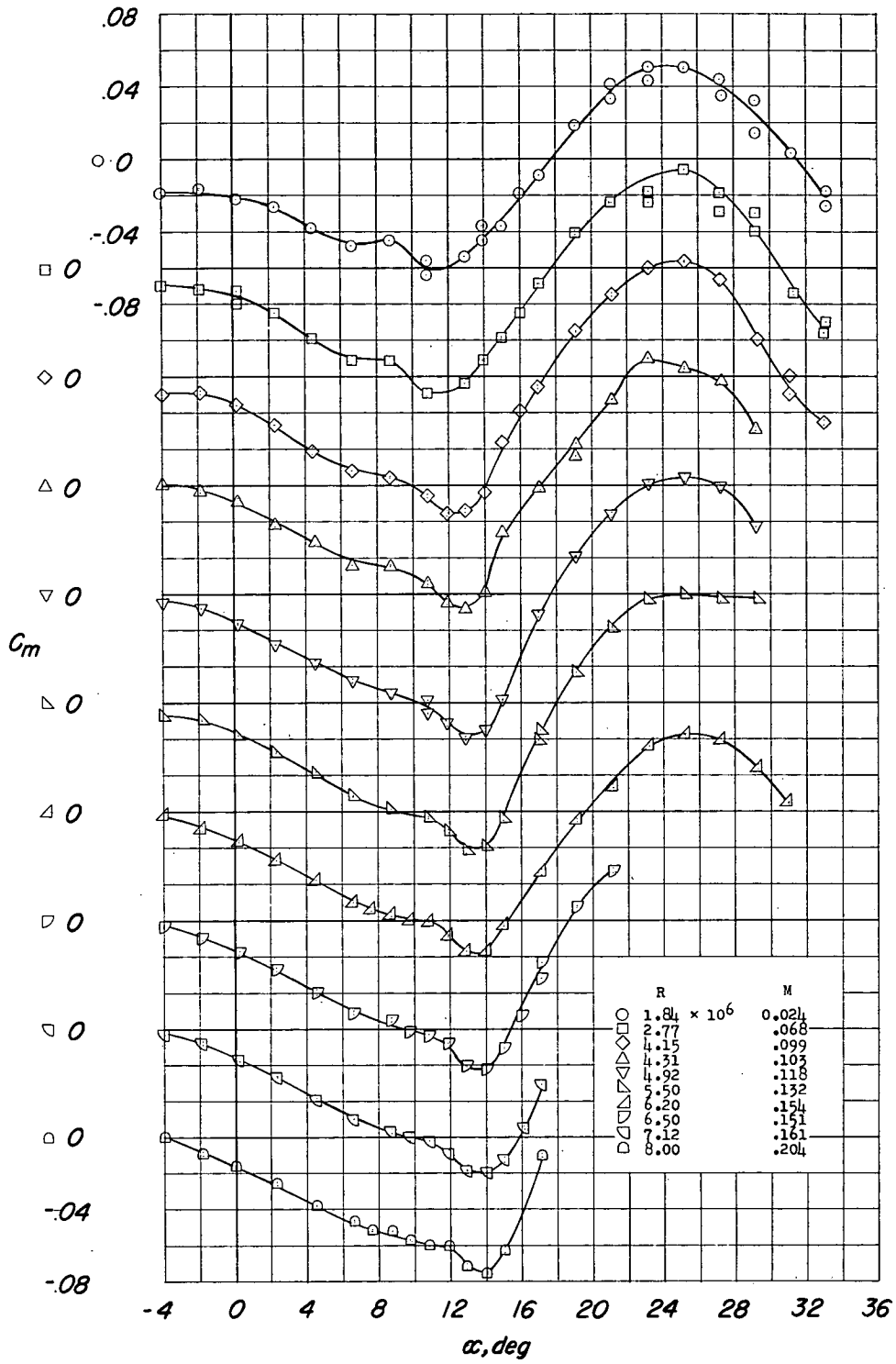

(d) C_m against α; pressure, 33 pounds per square inch.

Figure 8.- Concluded.

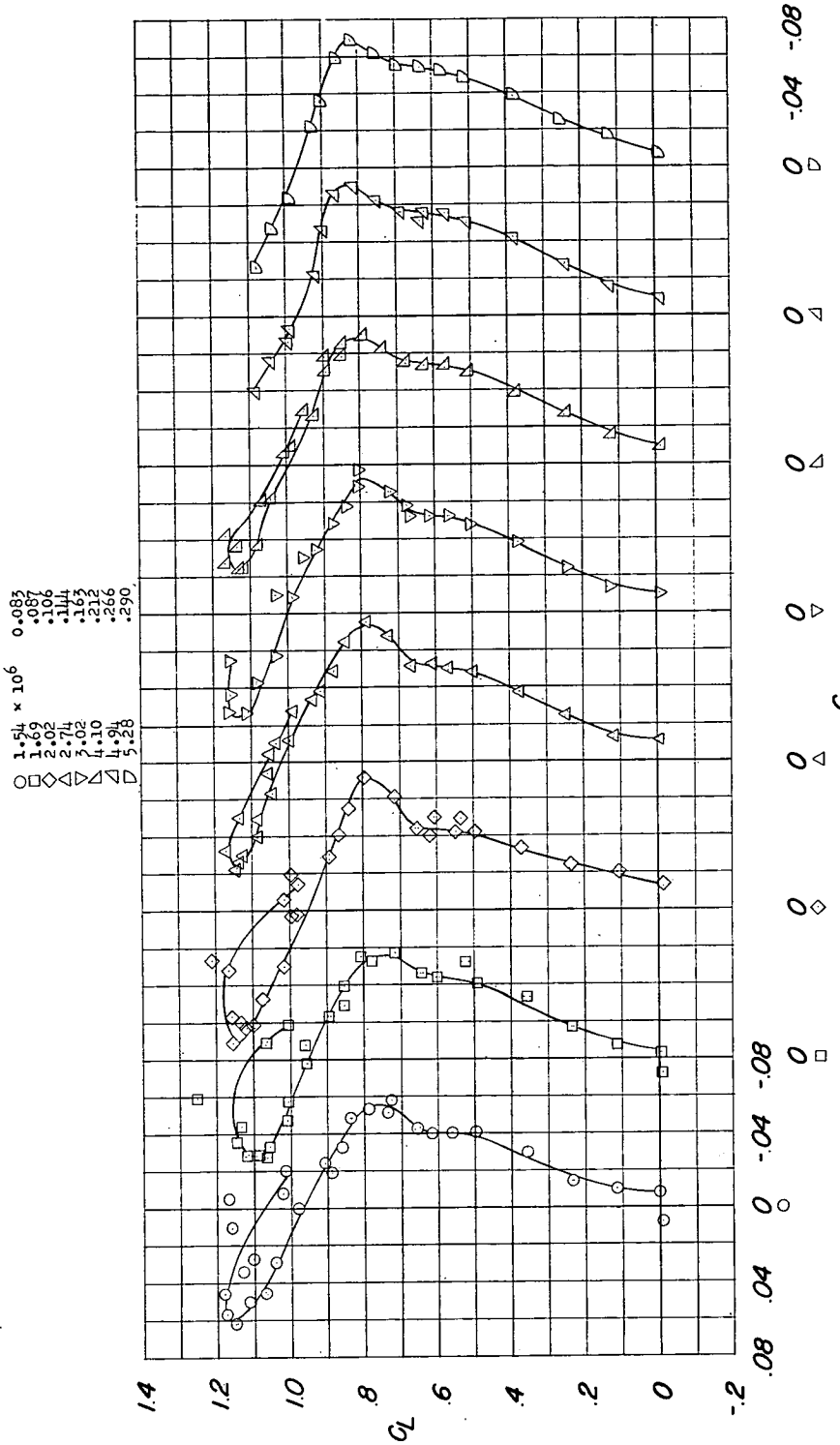

(a) Atmospheric pressure.

Figure 9.- Variation of pitching-moment coefficient with lift coefficient of a 45° sweptback wing. Aspect ratio, 5; C_{l_i} = 0.4; leading-edge radius, 0.0025c.

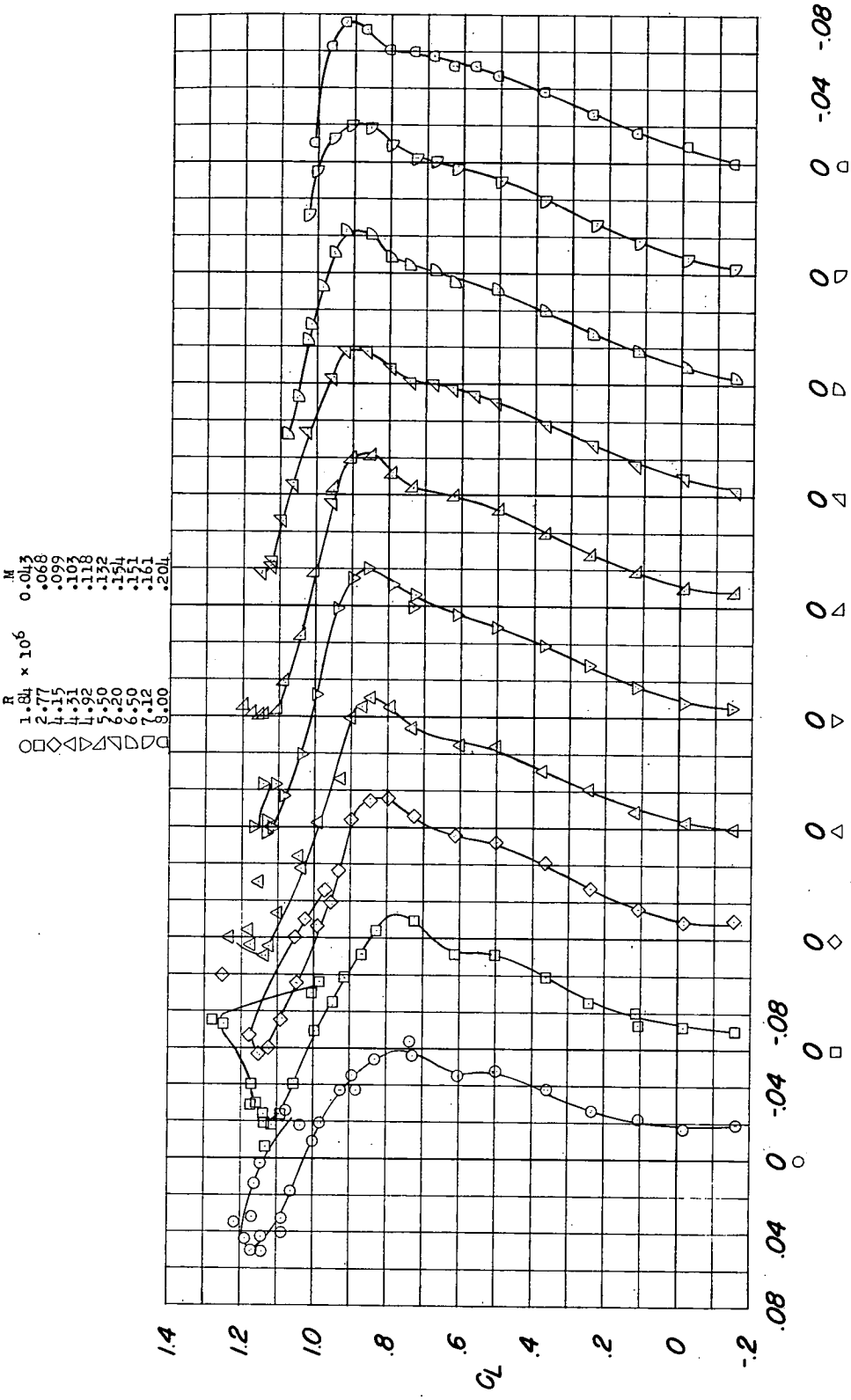

(b) Pressure, 33 pounds per square inch.

Figure 9.- Concluded.

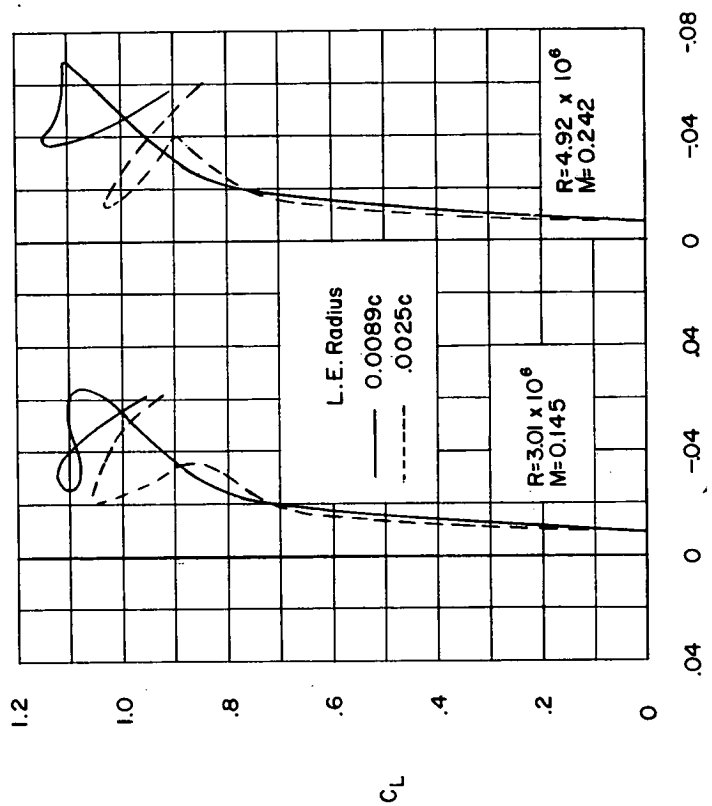

(a) Atmospheric pressure.

Figure 10.- Comparison of longitudinal stability characteristics of two 45° sweptback wings to show the influence of a change in leading-edge radius. Aspect ratio, 3; $C_{l_i} = 0.4$.

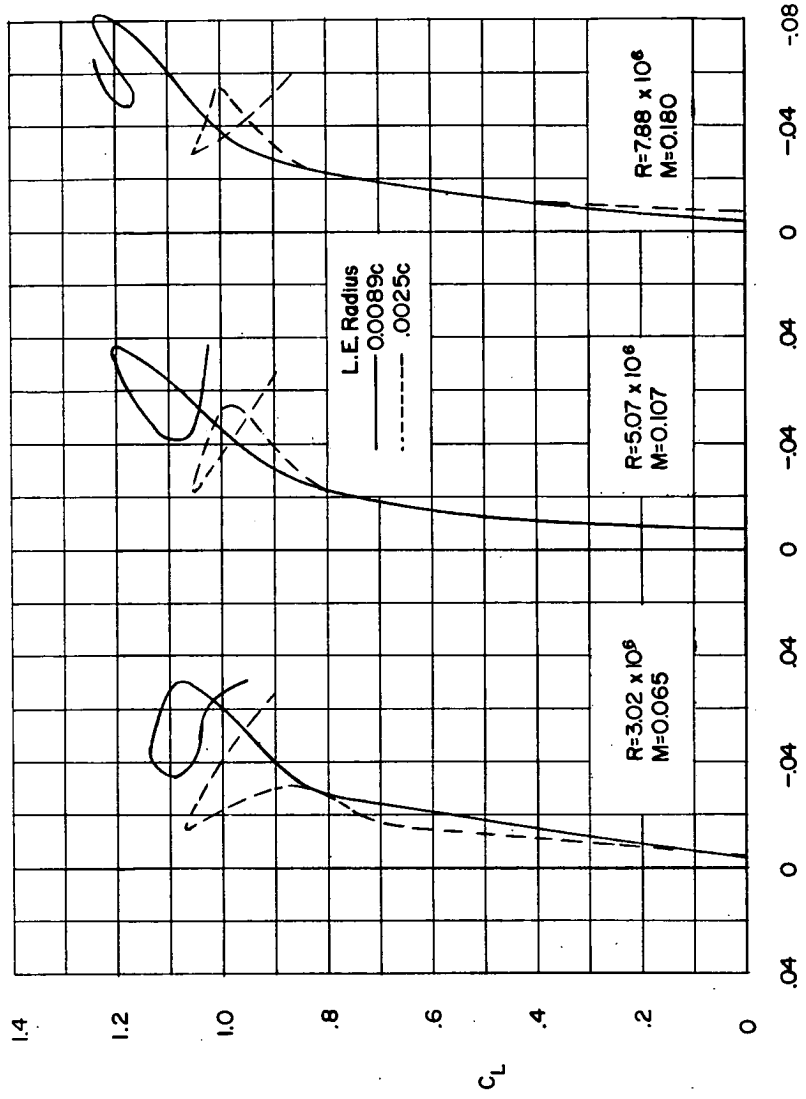

(b) Pressure, 33 pounds per square inch.

Figure 10.- Concluded.

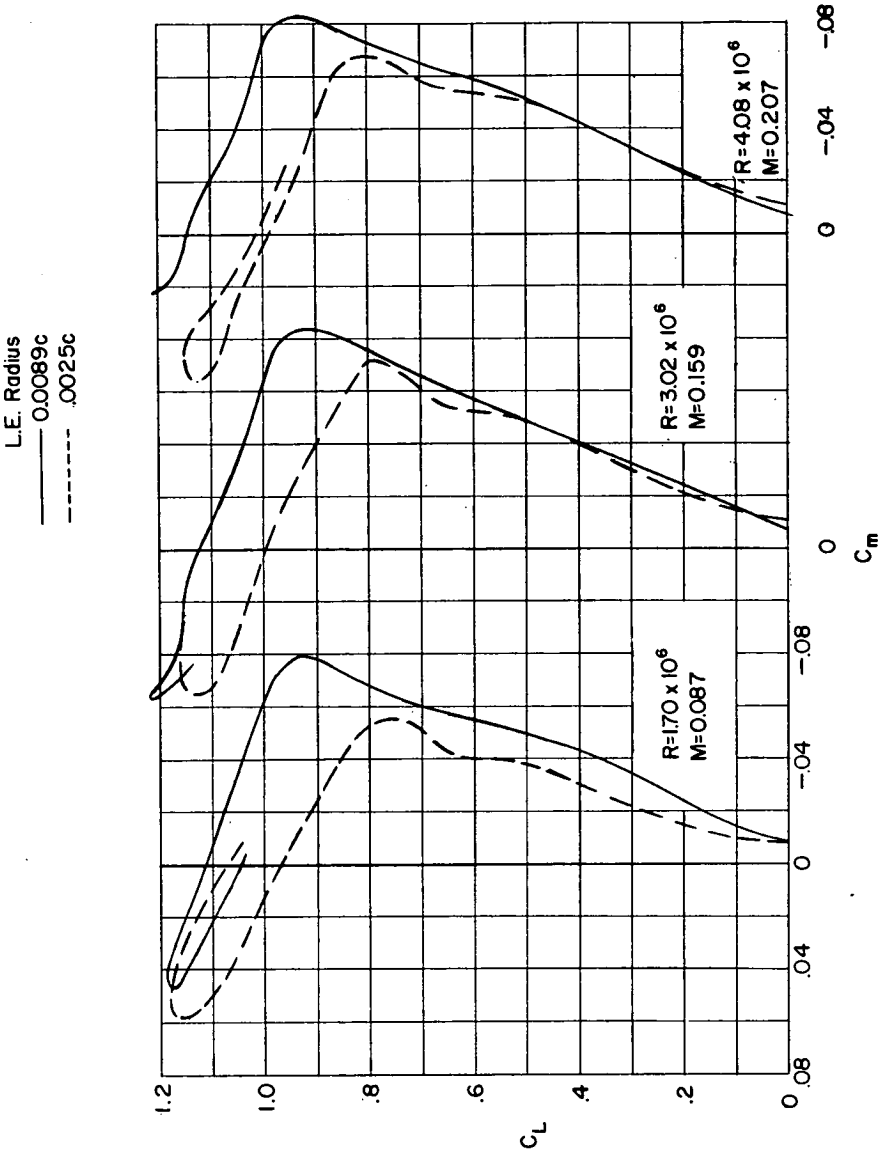

(a) Atmospheric pressure.

Figure 11.- Comparison of longitudinal stability characteristics of two 45° sweptback wings to show the influence of a change in leading-edge radius. Aspect ratio, 5; $C_{l_i} = 0.4$.

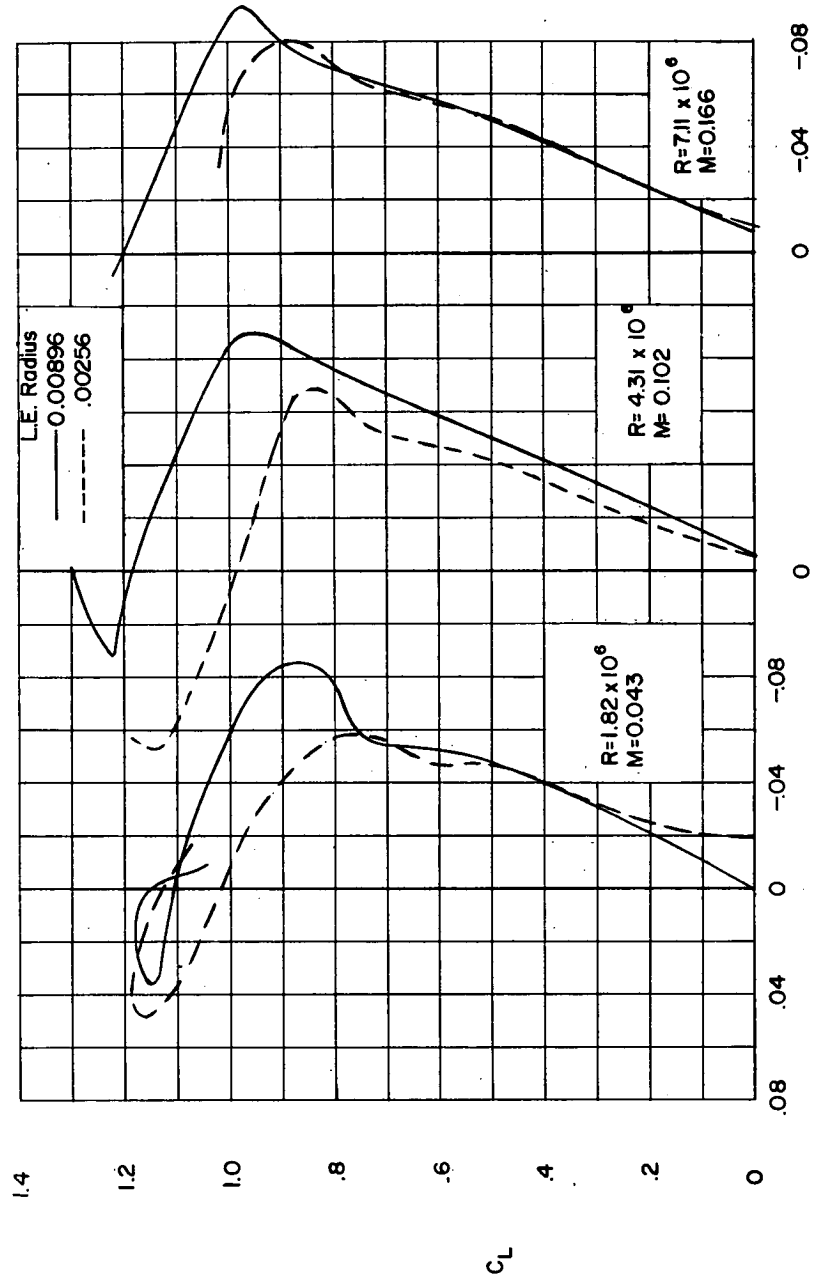

(b) Pressure, 33 pounds per square inch.

Figure 11.- Concluded.

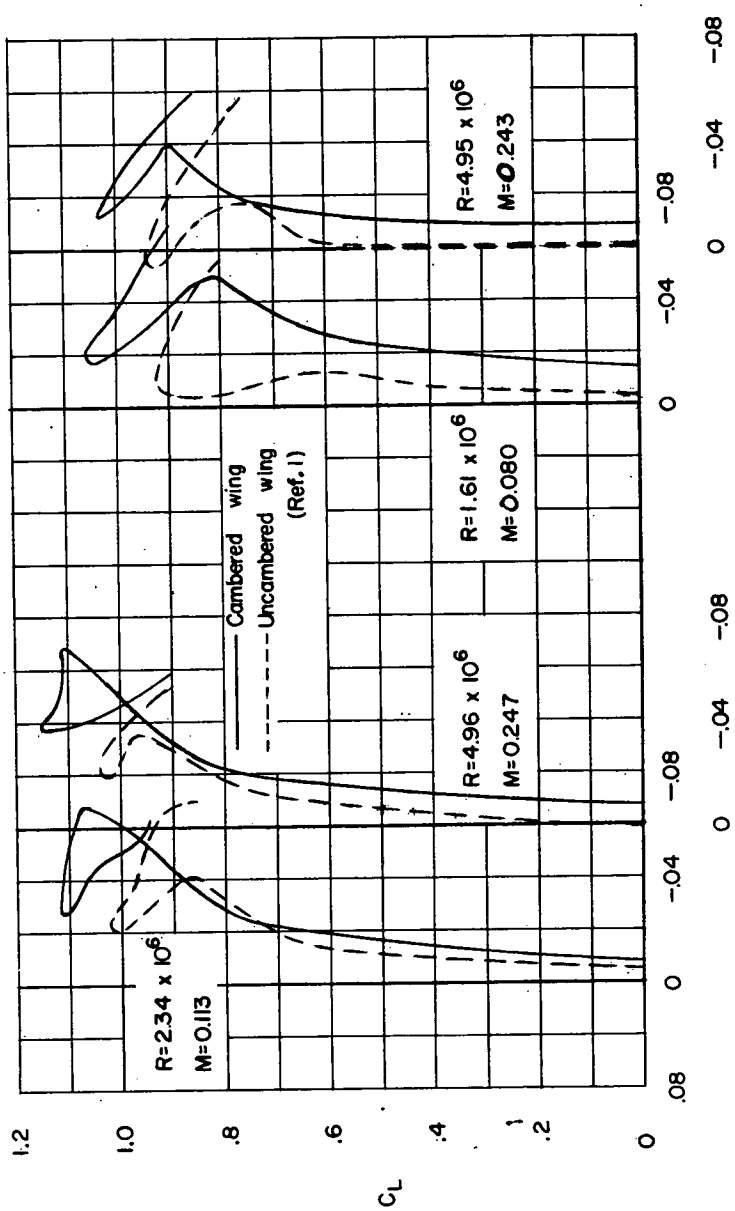

Leading-edge radius, 0.0089c Leading-edge radius, 0.0025c

(a) Atmospheric pressure.

Figure 12.- Effect of camber on the longitudinal stability characteristics of a 45° sweptback wing. Aspect ratio, 3.

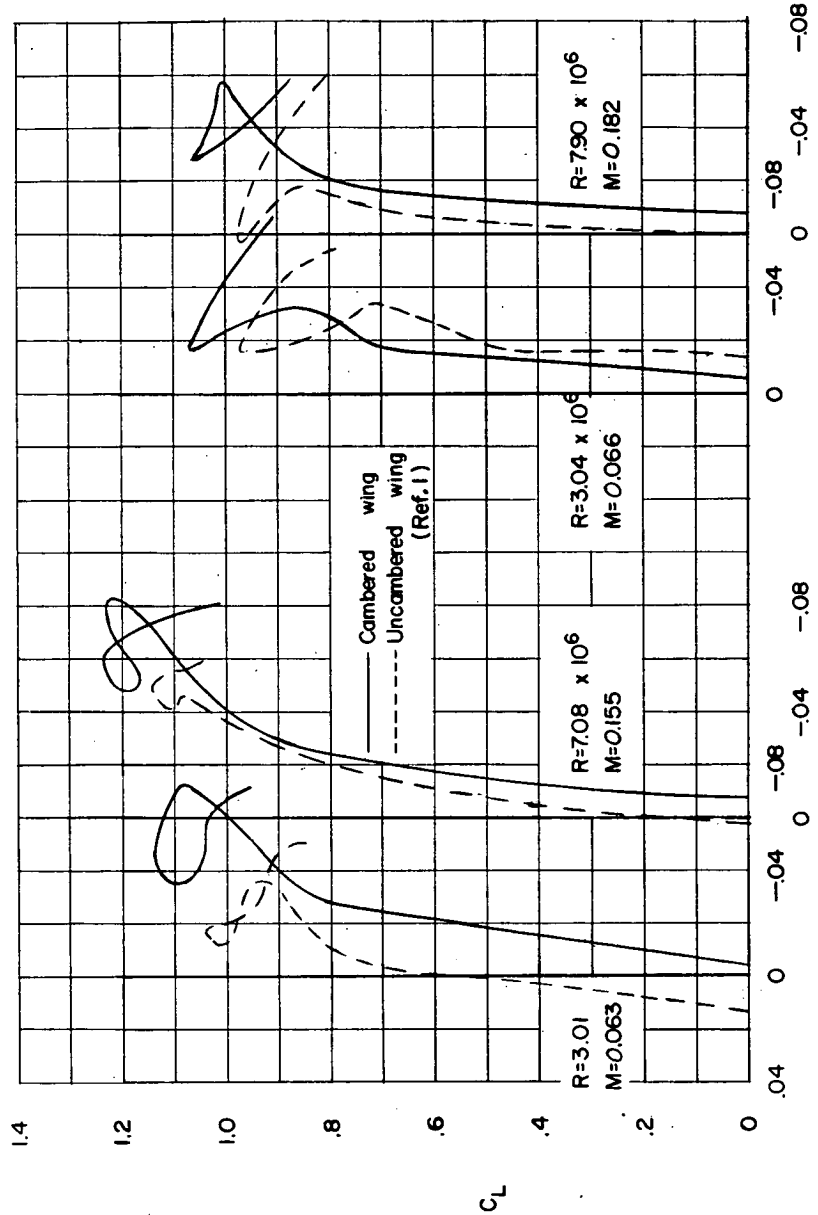

Leading-edge radius, 0.0089c Leading-edge radius, 0.0025c

(b) Pressure, 33 pounds per square inch.

Figure 12.- Concluded.

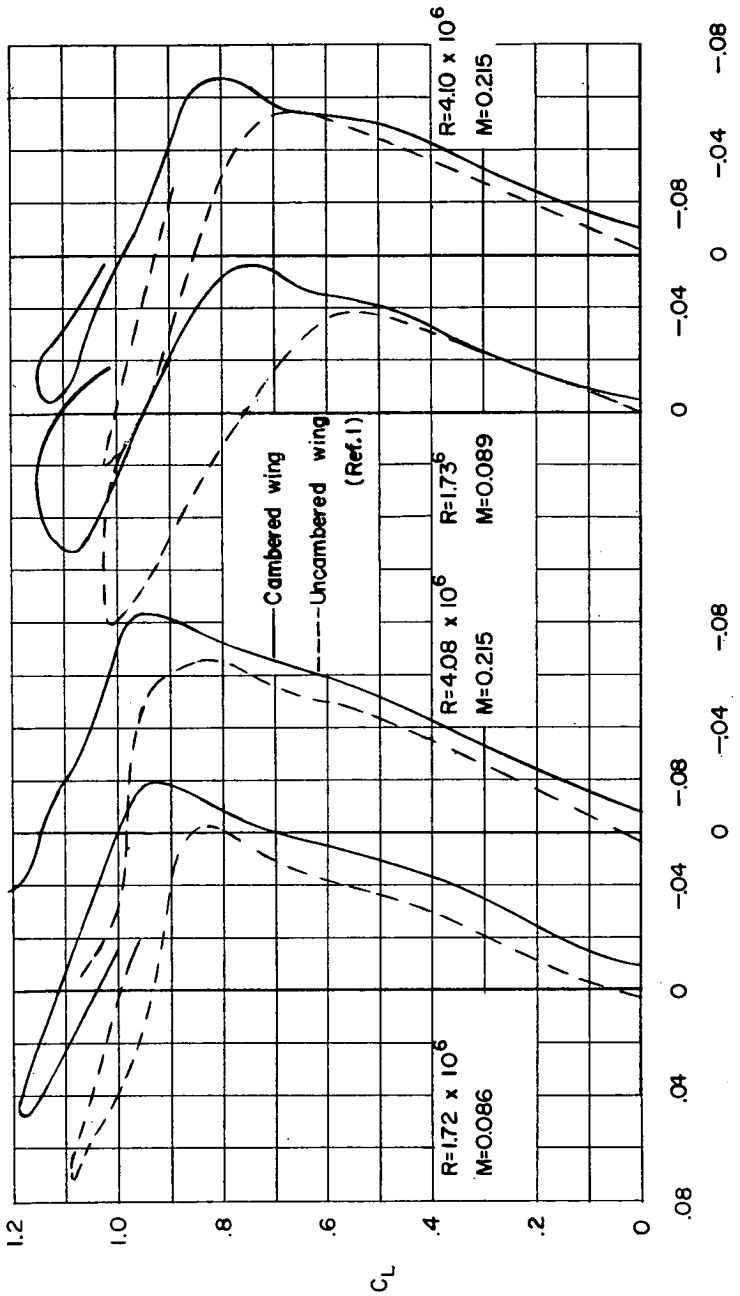

Leading-edge radius, 0.0089c Leading-edge radius, 0.0025c

(a) Atmospheric pressure.

Figure 13.- Effect of camber on the longitudinal stability characteristics of a 45° sweptback wing. Aspect ratio, 5.

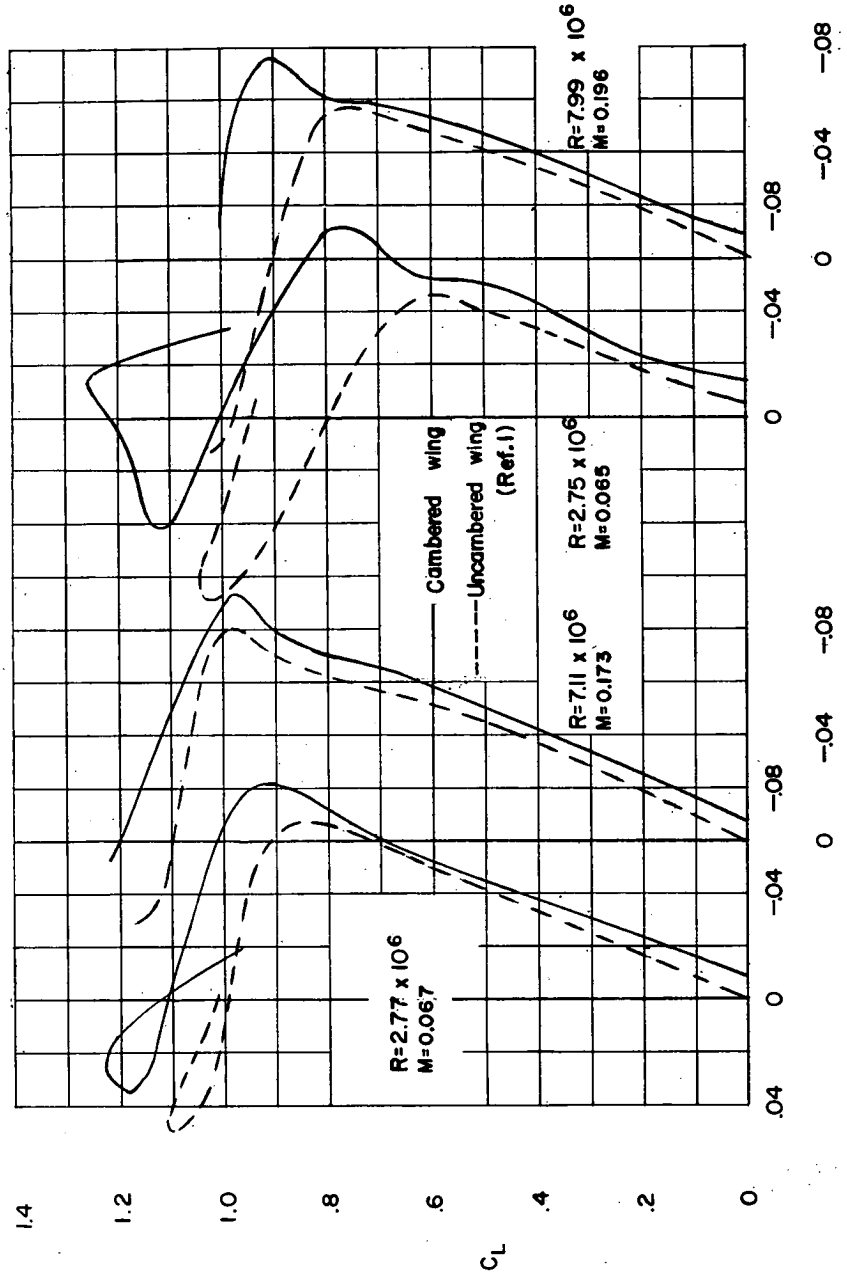

Leading-edge radius, 0.0089c Leading-edge radius, 0.0025c

(b) Pressure, 33 pounds per square inch.

Figure 13.- Concluded.

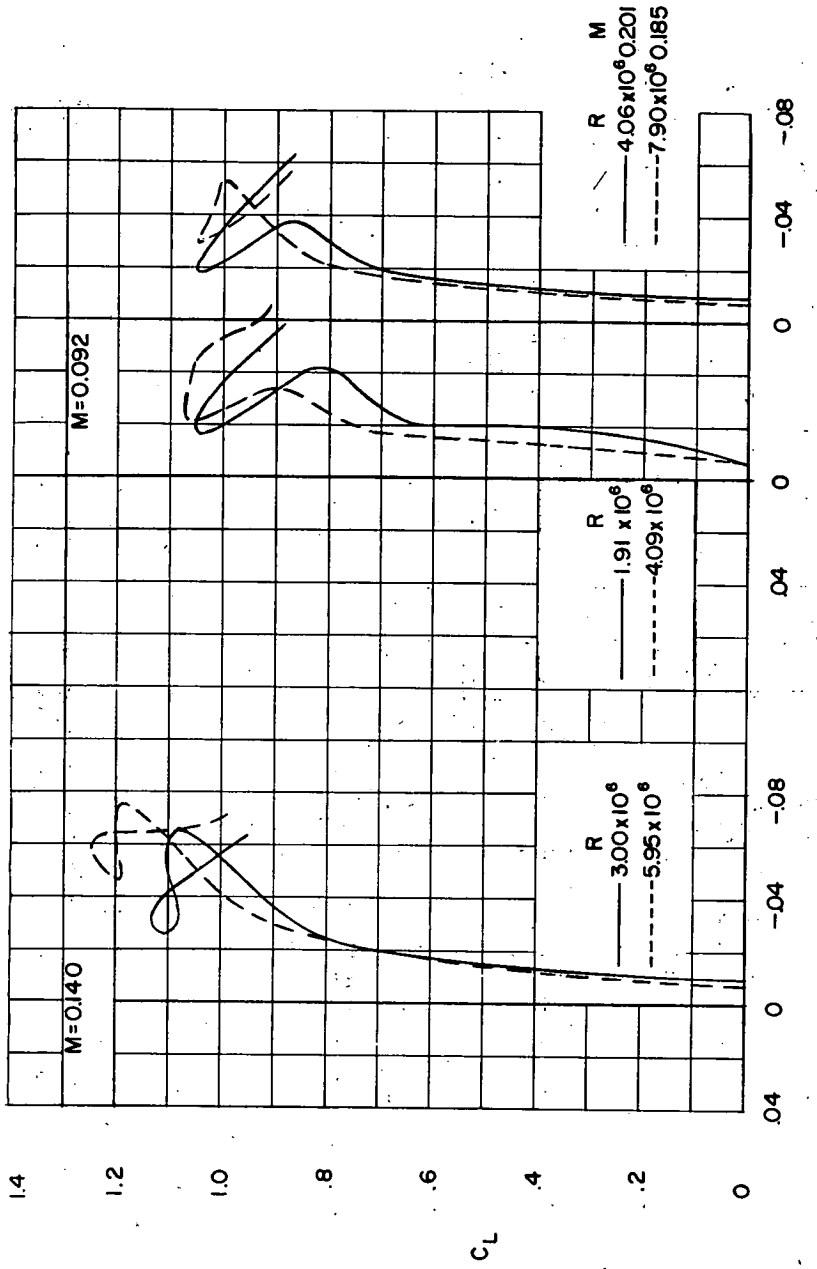

(a) Leading-edge radius, 0.0089c. (b) Leading-edge radius, 0.0025c.

Figure 14.- Comparison of longitudinal stability characteristics of two 45° sweptback wings at a constant Mach number to show the influence of Reynolds number. Aspect ratio, 3; $Cl_i = 0.4$.

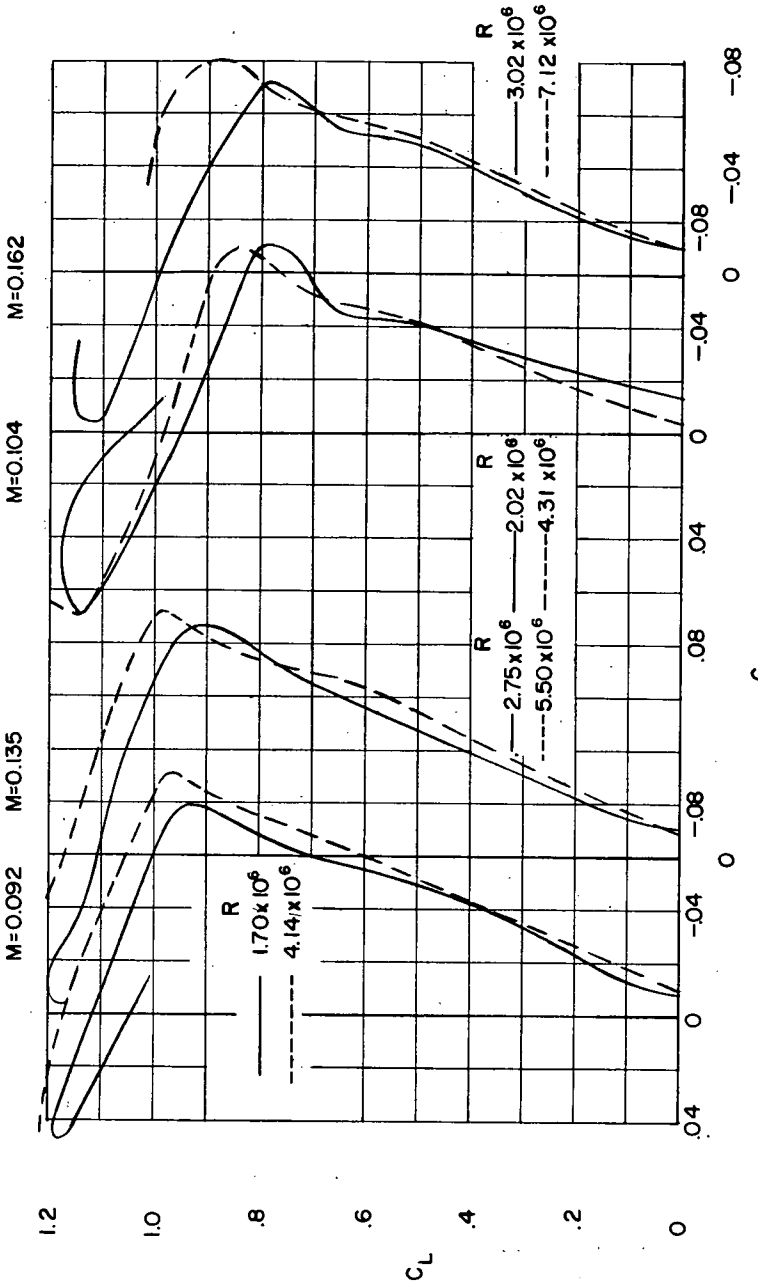

(a) Leading-edge radius, 0.0089c. (b) Leading-edge radius, 0.0025c.

Figure 15.- Comparison of longitudinal stability characteristics of two 45° sweptback wings at constant Mach numbers to show the influence of Reynolds number. Aspect ratio, 5; $C_{l_i} = 0.4$.

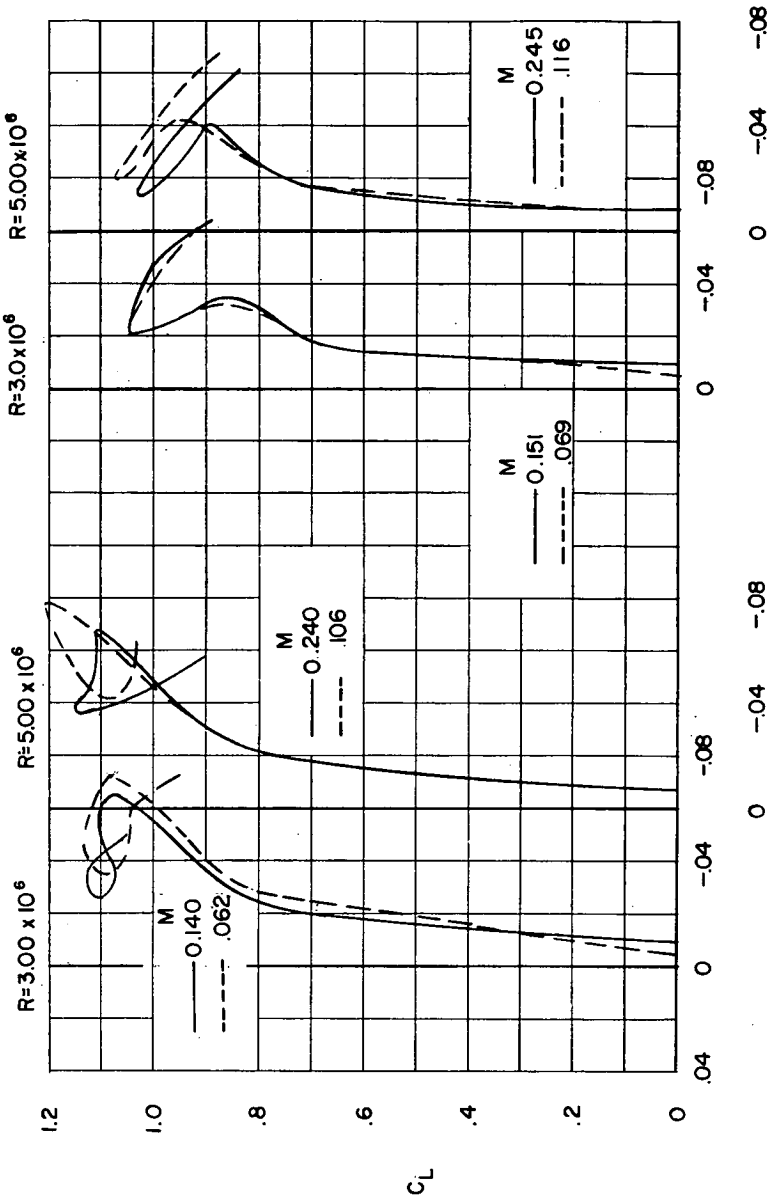

(a) Leading-edge radius, 0.0089c. (b) Leading-edge radius, 0.0025c.

Figure 16.- Comparison of longitudinal stability characteristics of two 45° sweptback wings at constant Reynolds number to show the influence of Mach number. Aspect ratio, 3; $C_{l_i} = 0.4$.

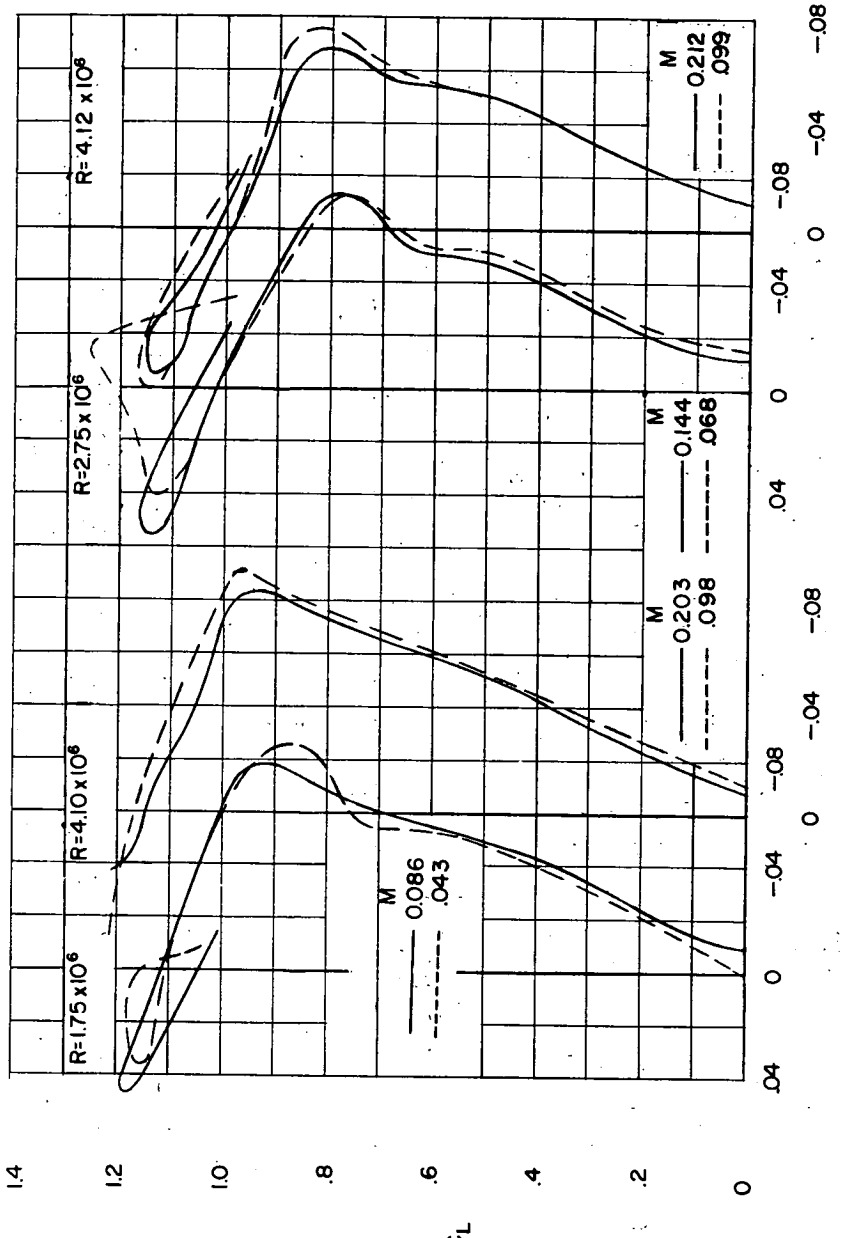

(a) Leading-edge radius, 0.0089c. (b) Leading-edge radius, 0.0025c.

Figure 17.- Comparison of longitudinal stability characteristics of two 45° sweptback wings at constant Reynolds number to show the influence of Mach number. Aspect ratio, 5.